PATTERNS OF RADAR ECHOES OF CONVECTIVE PRECIPITATION

HIGH PLAINS OF TEXAS, 1961

By

WAYNE CLYMA

Bachelor of Science

Oklahoma State University

Stillwater, Oklahoma

1958

Submitted to the faculty of the Graduate School of
the Oklahoma State University
in partial fulfillment of the requirements
for the degree of
MASTER OF SCIENCE
August, 1963

PATTERNS OF RADAR ECHOES OF CONVECTIVE PRECIPITATION,

HIGH PLAINS OF TEXAS, 1961

Thesis Approved:

F. R. Crow

Thesis Adviser

R. L. Nelson

Dean of the Graduate School

ACKNOWLEDGEMENT

The writer wishes to express his appreciation to all those who aided him in this investigation. Numerous individuals assisted by direct and indirect means.

The writer is indebted to the Soil and Water Conservation Research Division, Agricultural Research Service, U. S. Department of Agriculture, whose sponsorship of the research made this investigation possible and to Dr. J. R. Johnston, Chief, Southern Plains Branch, for his assistance.

Mr. W. O. Ree, Research Investigations Leader, Southern Plains Branch, furnished much helpful advice in planning this investigation.

The valuable guidance and encouragement of Professor F. R. Crow throughout this study is greatly appreciated.

The assistance of William E. Fry, Engineering Technician, Southern Plains Branch, in suggesting the utilization of the coordinate method of computing areas and collecting the data is acknowledged.

Appreciation is due Mr. D. K. McCool, Graduate Student, Agricultural Engineering Department, and Professors R. L. Caskey and R. D. McDole, Mathematics Department, who assisted in various ways in the development of the method for computing the centroid.

Recognition should be given Professor Herbert Kershaw, Jr., Meteorology Department, and Mr. Arlin D. Nicks, Agricultural Engineer, Southern Plains Branch, for their assistance in matters concerning meteorology and radar theory and practice.

The assistance of the U. S. Weather Bureau, National Weather Records Center, Ashville, North Carolina, which made available radar operator's logs on file, is appreciated.

The writer wishes to acknowledge the assistance of the Amarillo Weather Bureau, from whom the film was obtained. The cooperation of various personnel of the Amarillo Weather Bureau, Amarillo, Texas, by answering questions and making suggestions, aided this investigation.

The writer is indebted to Mr. Glen N. Williams, Programmer, Data Processing Center, Texas Engineering Experiment Station, College Station, Texas, for programming a computer to make the computations for analyzing the data.

Acknowledgment is due Mr. C. E. Van Doren, Superintendent, and the staff of the Southwestern Great Plains Field Station, Bushland, Texas, for their assistance.

To my wife, Marjorie Marie, and son, Gary Wayne, for their inspiration and encouragement, this thesis is dedicated.

TABLE OF CONTENTS

LIST OF TABLES

LIST OF FIGURES

Figure Page

CHAPTER I

INTRODUCTION

Results from studies by other research workers indicate that radar can be used to increase the knowledge of precipitation patterns for an area. A study of radar echoes would result in data concerning their mean, median, and extreme characteristics. Also, a computer may be used to speed the interpretation of radar data, if the characteristics of the radar echo can be presented in digital form.

Having access to film from the U. S. Weather Bureau at Amarillo, Texas gave the opportunity to make a study of radar echoes for the High Plains of Texas. Many of the storms that contribute precipitation to the High Plains are believed to be multicellular, and scattered rain gages do not provide an accurate characterization of the areal distribution of precipitation. Radar scope pictures, because of their complete areal coverage, provide a better characterization of the precipitation patterns.

This thesis presents the results of a study of the characteristics of radar echoes of convective precipitation for the High Plains of Texas. Methods revised and developed by the writer to facilitate data collection and analysis are also presented.

CHAPTER II

OBJECTIVES

The objectives of this research project were as follows:

1. Develop a procedure for converting to digital form radar echoes depicted on the plan-position indicator scope to facilitate computation and summarization of their characteristics by a high speed computer.
2. Determine the initiation, growth, and dissipation characteristics of radar echoes of isolated or randomly occurring convective precipitation for the High Plains of Texas.

CHAPTER III

REVIEW OF LITERATURE

Principles of Radar Operation

Before the potential applications of radar to hydrology can be developed, some understanding of the principles of radar operation is necessary. Thus, a brief review of the principles of radar operation and precipitation detection will be presented.

A radar set consists basically of a transmitter, which produces radio energy; an antenna, which radiates the energy and intercepts the returned energy; a receiver, which detects, amplifies, and transforms the received signal into video form; and an indicator, on which the returned signals can be displayed. A schematic diagram of such a radar set is presented in Figure 1. Most radar sets use a single antenna to transmit and receive the signal. An automatic switch is used to shut off the receiver during the short interval that the transmitter is operating.

Several types of indicators are available for use in a radar set. The indicator used for this study was the plan-position indicator (PPI). A schematic diagram of a PPI scope is presented in Figure 2.

The Radar Equation

Several authors (1, 2, 3) have presented the theoretical considerations on which the equation describing the detection of meteorological

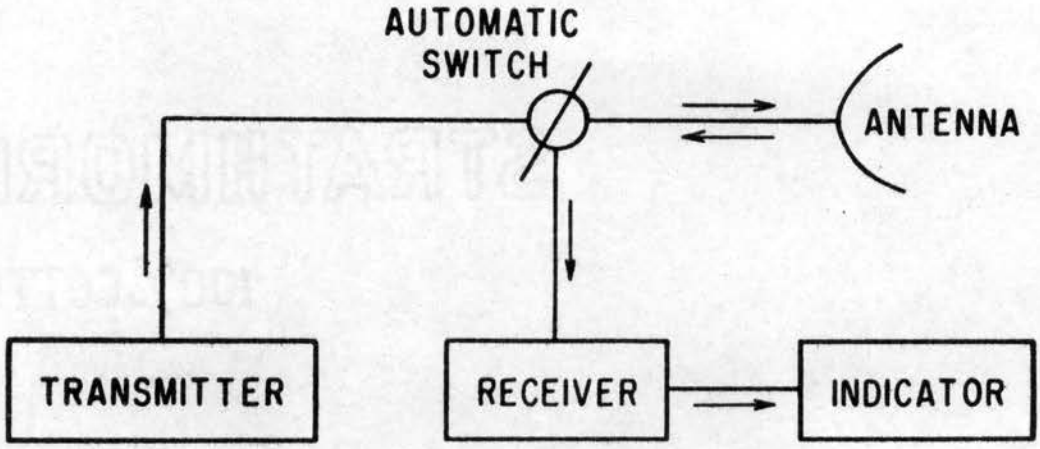

Figure 1. Block diagram of a radar set.

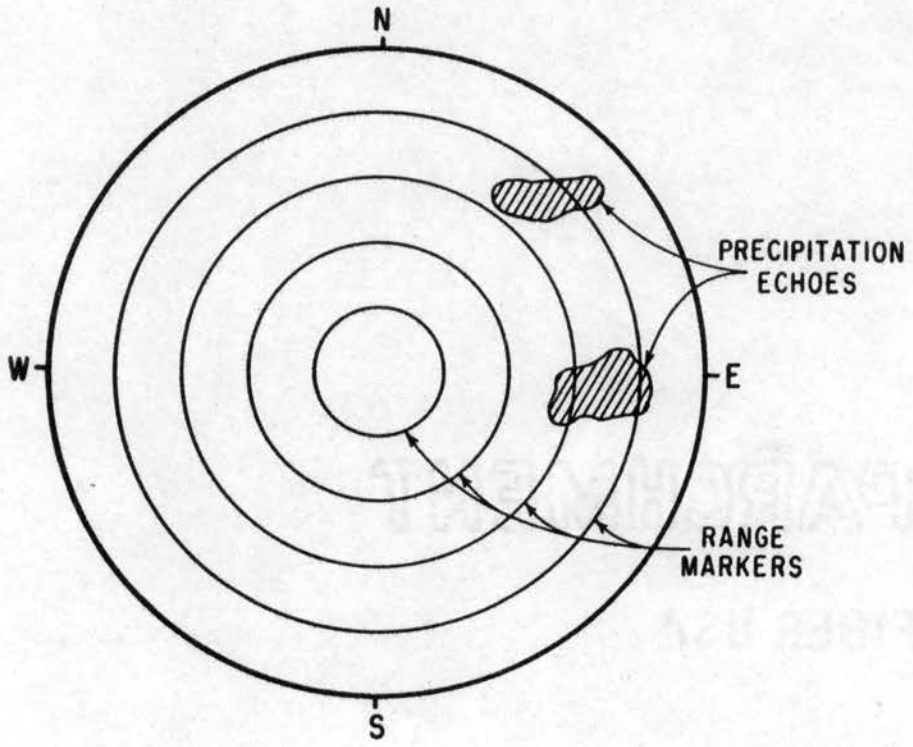

Figure 2. The plan-position indicator (PPI) scope.

phenomena is based. The equation presented by these authors describing the average power returned to a radar set by randomly distributed particles in space is:

$$\overline{P}_r = \frac{\pi^5 P_t \theta \phi h A_p^2 |K|^2 z}{72 \lambda^6 r^2} \quad [1]$$

$\overline{P}_r$ is the average value of the power received at the radar

P_t is the power transmitted by the radar

θ is the horizontal width of the beam in radians

ϕ is the vertical width of the beam in radians

h is the pulse length

A_p is the apertural area of the antenna

$|K|^2$ is the complex index of refraction and for water drops is equal to approximately 0.93 and for ice particles 0.19

z is the symbol to designate $\sum_{\text{Vol.}} D_i^6$ and is the "reflectivity factor"

$\sum_{\text{Vol.}} D_i^6$ is the sum of the total backscattering of all particles within the volume intercepting the radar beam

r is the range of the target particles intercepting the beam

λ is the wave length of radiation

Certain factors in equation [1] are constants for a particular radar. They can be evaluated and equated to a constant C_1, where:

$$C_1 = \frac{\pi^5 P_t \theta \phi h A_p |K|^2}{72 \lambda^6} \quad [2]$$

Equation [1] then becomes:

$$\overline{P}_r = \frac{C_1 z}{r^2} \quad [3]$$

Thus, the average power received by the radar (the ability of the radar

to detect water droplets) is largely dependent on the size of the droplets and the range at which they occur.

Equation [1] is the general equation for the average power received by a radar. However, the equation does not hold for certain conditions. For example, if the beam is wider than the group of particles intercepted and only part of the beam is filled, equation [1] must be modified by a factor, Ψ, which is the fraction of the cross-sectional area of the beam filled. (2). When the radar operates at short wave lengths, attenuation may occur. Attenuation is the reduction of power received at the radar by the absorption and scattering effects of the medium through which the electro-magnetic waves travel in reaching the target. (2). Attenuation is not a problem when wave lengths of 10 cm. or longer are used. (1, 2, 3, 4, 5).

Applications of Radar to Hydrology

The identity of the first person to decide that certain radar echoes were of meteorological origin is not known, but use of radar in meteorology is known to have occurred as early as 1942. (1). The basic theory explaining the occurrence of weather echoes was developed by Ryde (6) using Rayleigh's (7) and Mie's (8) theory of the scattering of electromagnetic waves. A summary of the early work in the field of radar meteorology has been made by Kerr. (9). More recent summaries can be found in Marshall et al. (1) and Nupen. (10). Proceedings of the Weather Radar Conferences are excellent sources of literature on the application of radar to weather and precipitation.

The applications of radar to hydrology are varied. There is no unique relationship between the signal received by a radar and quantitative rainfall. Therefore, many applications have been concerned with additional information that can be gained by using radar to supplement rain gages. Other applications have dealt with the development of empirical relationships between rainfall and the signal received.

Truppi (11) used radar in conjunction with rain gages to increase the knowledge of precipitation patterns. His study area was 144 miles square and was broken down into grids that were 12 miles square. At intervals of time he listed the squares containing echoes. Then various types of correlations were made between rainfall and the number of echoes within the grid. The resulting pattern of precipitation using the radar and rain gages provided more detail than the rain gages alone could supply.

Flood forecasting with radar has been practiced by Tarble. (12). Multiple exposure photographs were used to determine location and areal extent of stationary cells. An occasional rain gage was used to determine the magnitude of rainfall associated with a particular echo return. Flood areas were predicted from the combination of radar photographs and rainfall measurements.

Clark (13) studied convective precipitation patterns for south Texas and used computer techniques to assist in summarizing the data. He used an azimuth and distance to the apparent echo center to locate the echo. Total distance traveled, velocity, and duration were studied.

Changnon (14) used radar for a climatological study of squall lines and other types of precipitation lines. Some characteristics that he studied were: (1) direction of movement, (2) speed of movement, (3) dimensions of lines, (4) duration, (5) time of occurrence, (6) daily and monthly line frequencies, and (7) location of line centers. Mean, median, and extreme values for the above properties were computed based on the mean values of each line determined from all measurements during the line duration.

Further development of computer science to speed the interpretation of the volumes of data radar accumulates was made by Truppi. (15). Radar displays of precipitation echoes were transformed to a digital form using an analogue to digital converter. Projected images of the PPI scope were overlaid with a grid. The grid squares containing echoes were identified by a four digit output from the converter. The digital outputs were placed on cards for further computations by high speed computers.

Geographic and Precipitation Characteristics of the High Plains

The Texas High Plains, an area of approximately 22 million acres, includes most of the Texas Panhandle (Figure 3). This area is a plateau bounded on all sides by a rather abrupt escarpment. The surface is nearly level with an average slope of approximately 10 feet per mile from the northwest to the southeast. Its topography is characterized by numerous enclosed basins, or playas, with only a small portion of the area drained by streams.

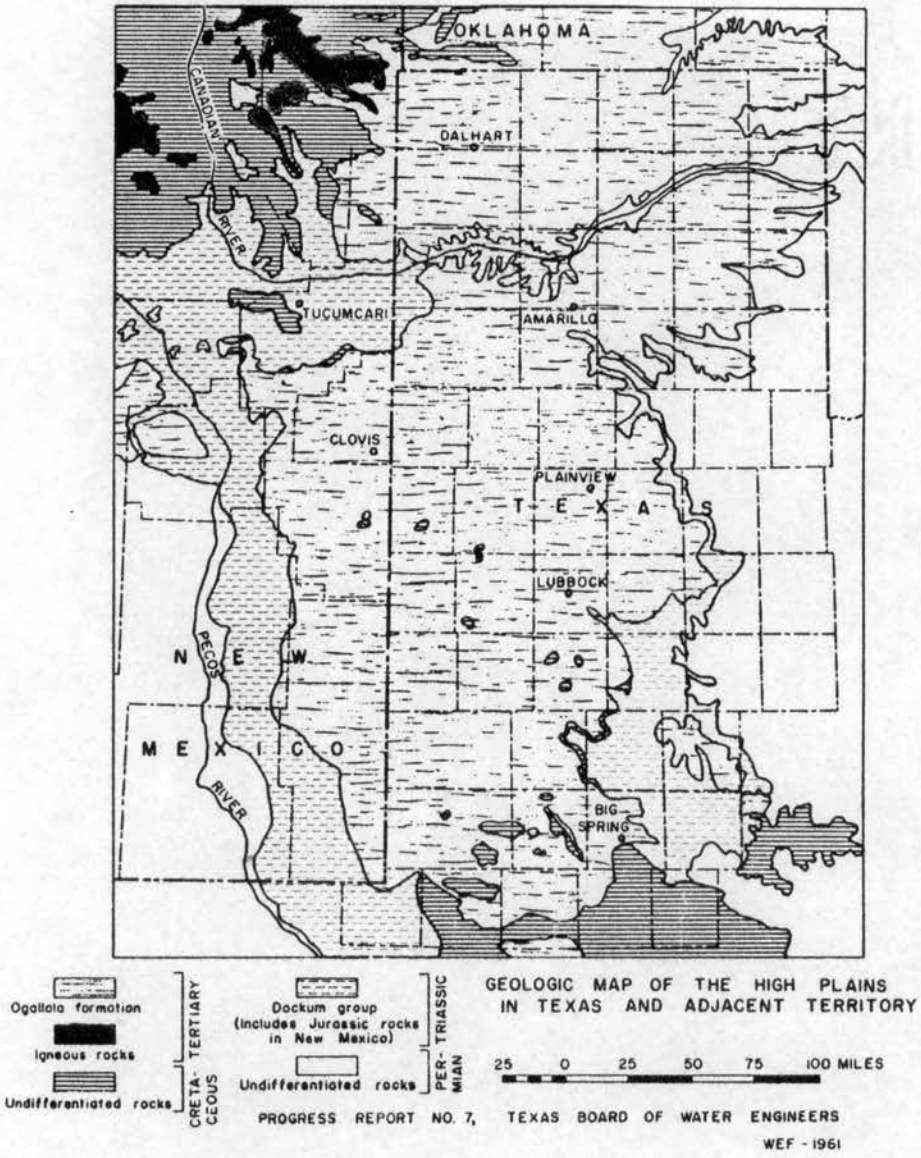

Figure 3. The High Plains of Texas and adjacent territory.

The climate of the High Plains is classed as semiarid. Average annual precipitation for the area decreases from south to north and from east to west. Precipitation ranges from 18.3 inches at Big Spring, Texas, in the south to 17.9 inches at Dalhart, Texas, in the north. (16). The east-west range is from 21.9 inches at Shamrock, Texas, (16) to 16.8 inches at Tucumcari, New Mexico. (17). Rainfall for the area tends to have a summer peak (Figure 4). For example, at Amarillo, Texas, 51 percent of the annual precipitation comes during June through September. (18).

Moisture for rainfall for the High Plains is predominantly tropical maritime and is supplied principally from the Gulf of Mexico. Two triggers for precipitation that falls on the area are localized heating, which results in convective thunderstorms, and polar fronts.

Convective thunderstorms may furnish appreciable rainfall to the area. These thunderstorms produce precipitation characterized by its relatively small areal extent and vary from a trace to several inches of rainfall. Usually this type of precipitation is not of great hydrologic importance. However, the topography of the High Plains makes the area an exception. The storms result in appreciable amounts of runoff as the closed basins have drainage areas of only a few acres to normally less than 3 square miles. This is because the runoff is contained in the basin, accumulates in the low spot, and cannot spread over larger areas to reduce the runoff volume per unit area.

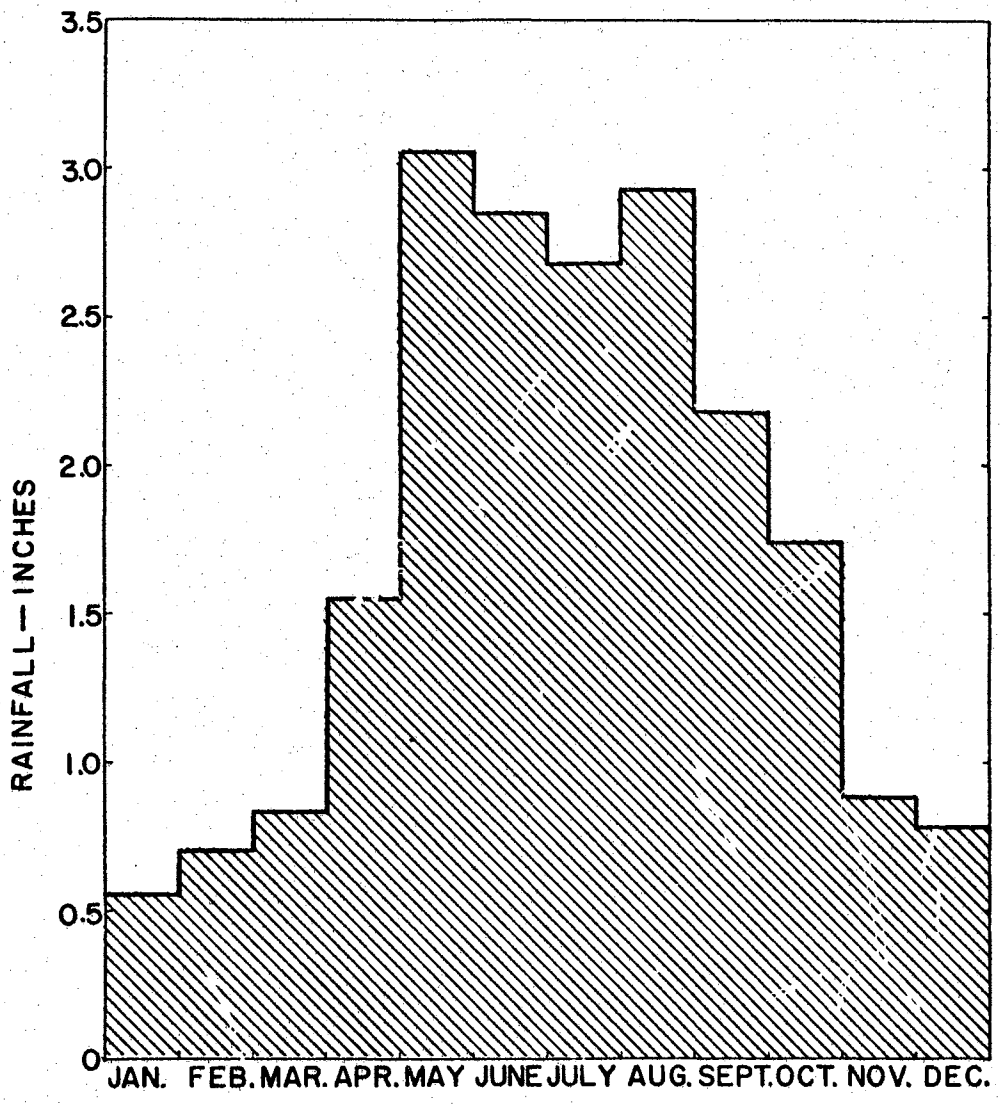

Figure 4. Average monthly rainfall at Amarillo, Texas.

CHAPTER IV

PROCEDURE

Selection of Study Area

To study convective precipitation patterns for the High Plains of Texas, a portion of the area was selected. Thus, the High Plains was assumed to be approximately meteorologically homogeneous. Any subsample of the area would be representative of the total area. Any meteorological heterogeneity that may exist would be reflected by a small uniform change in climatological characteristics from one location to another. The radar echoes of precipitation were assumed to occur randomly over the High Plains. These assumptions permit a study of only a portion of the area.

The sample area selected was bounded by two east-west lines 25 miles to the south and 25 miles to the north of an east-west line through Kress, Texas. The eastern and western boundaries were defined by two north-south lines 25 miles past the eastern and western edges of the escarpment. The boundaries are shown in Figure 5.

The sample area location was selected for the following reasons:

1. It was approximately centrally located in the High Plains from north to south.
2. It was about at the widest east-west point of the High Plains.
3. It was far enough from the radar site that normal ground clutter did not interfere with the tracking of precipitation echoes.

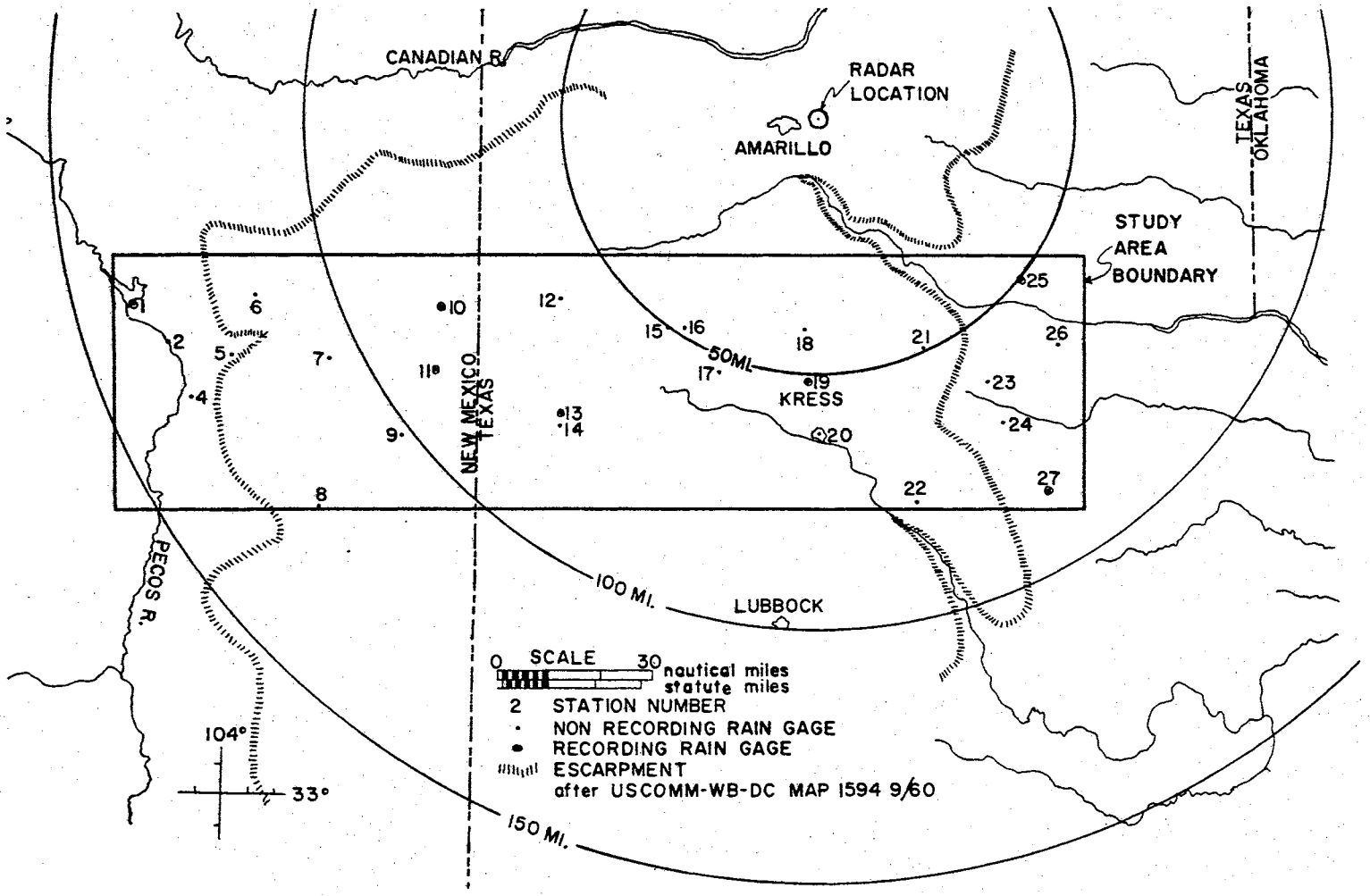

Figure 5. Boundaries of the sample area and rain gage locations.

Development of Procedure for Computing Echo Area and Centroid by Coordinates

In hydrologic studies, the location and area of a precipitation echo must be known with precision because this is the area of potential runoff. Several authors have studied the occurrence of radar echoes. They have employed either grid coordinates, composites of echo tracings, or planimetering to determine echo areas. Accurate determination of echo location and area by these procedures is laborious. Simplification of the procedures, to reduce data processing labor, results in undesirable approximations of location and area. Thus, the following procedures were devised to determine the area and the centroid (center of mass) of precipitation echoes.

From analytic geometry it can be shown that the area of any polygon can be determined from the coordinates of points bounding the figure. Several systematic procedures are available for computing the area of a polygon (such as Figure 6). One method considers the polygon as a series of trapezoids each with one side on the Y axis.

To further aid in systematic area computations for a polygon, the trapezoids may be divided into rectangular and triangular areas. The area of the trapezoid 1, 2, y_2, y_1, 1 in Figure 6 is:

for the rectangle

$$A_r = (y_2-y_1)\, x_1 \qquad [4]$$

for the triangle

$$A_t = (y_2-y_1)\, \frac{(x_2-x_1)}{2} \qquad [5]$$

The area of the trapezoid would be

$$A_T = A_r + A_t \qquad [6a]$$

or

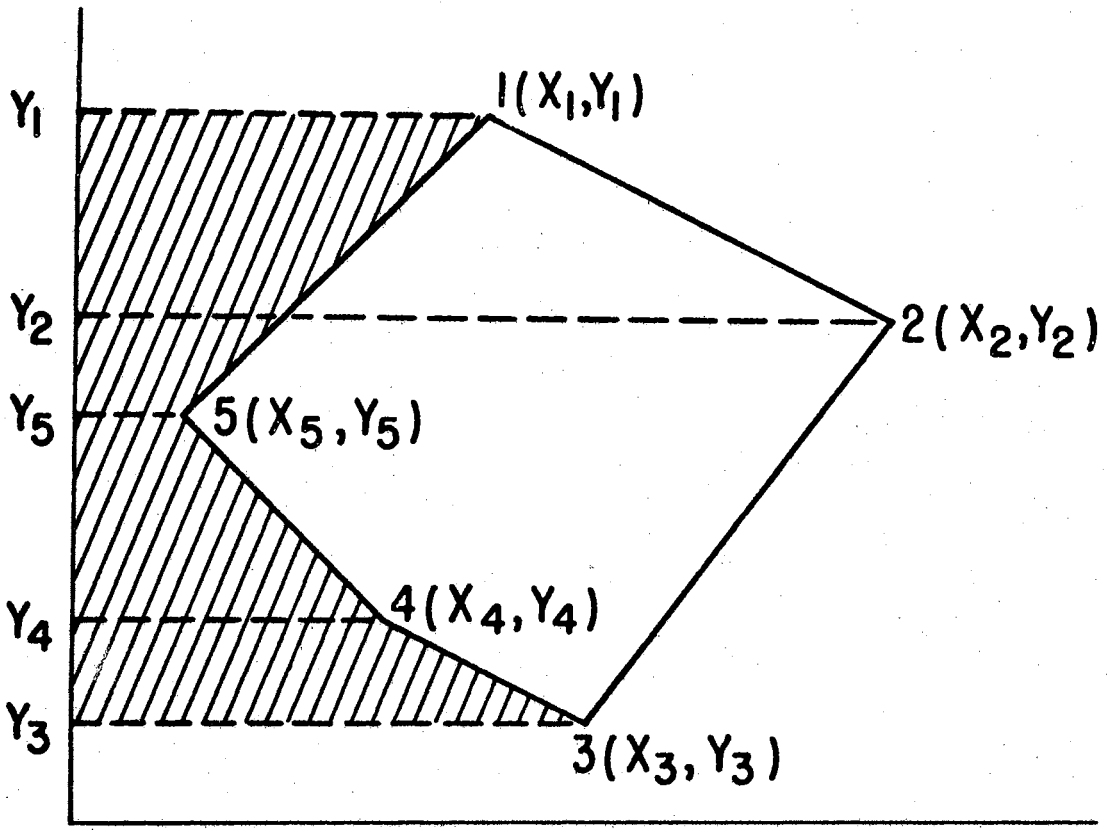

Figure 6. An N-sided polygon (N=5).

$$A_T = (y_2-y_1)\, x_1 + (y_2-y_1)\, \frac{(x_2-x_1)}{2} \qquad [6b]$$

The area for the polygon in Figure 6 would then be the algebraic sum of the area of the trapezoids.

$$\begin{aligned} A_y = {} & (y_2-y_1)\, x_1 + (y_2-y_1)\, \frac{(x_2-x_1)}{2} \\ & + (y_3-y_2)\, x_2 + (y_3-y_2)\, \frac{(x_3-x_2)}{2} \\ & + (y_4-y_3)\, x_3 + (y_4-y_3)\, \frac{(x_4-x_3)}{2} \\ & + (y_5-y_4)\, x_4 + (y_5-y_4)\, \frac{(x_5-x_4)}{2} \\ & + (y_1-y_5)\, x_5 + (y_1-y_5)\, \frac{(x_1-x_5)}{2} \end{aligned} \qquad [7]$$

Equation [7] can be generalized for any N-sided polygon such that the area:

$$A_y = \sum_{n=1}^{N+1} (\Delta y_n x_n + \Delta y_n \frac{\Delta x_n}{2}) \qquad [8]$$

Where:

A_y is the total area of any N-sided polygon

y subscript denotes the trapezoids have one side on the y axis

N is the number of (x,y) coordinates used in bounding the area and N+1 is also 1

$$\Delta x_n = x_{n+1} - x_n \quad (n = 1, 2, 3, \ldots, N, N+1) \qquad [9]$$

$$\Delta y_n = y_{n+1} - y_n \quad (n = 1, 2, 3, \ldots, N, N+1). \qquad [10]$$

The area A_y will have a positive or negative algebraic value depending on whether the polygon is traversed in a counterclockwise or clockwise direction. In any event we may use the absolute value of A_y.

$$A_y = \left| \sum_{n=1}^{N+1} (\Delta y_n x_n + \frac{\Delta y_n \Delta x_n}{2}) \right| \qquad [8a]$$

The centroid of a plane surface is described as a point that corresponds to the center of gravity of a thin homogeneous plate of the same area and shape. Methods for determining the centroids of symmetrical figures or figures for which the boundaries can be represented as an equation have been presented many times. To the writer's present knowledge, the following method for determining the centroid of an N-sided polygon has not been presented.

The moment of an area with respect to an axis has been defined as the area of the figure times the normal distance from the axis to the centroid of the area. Thus

$$M_y = A\bar{X} \qquad [11]$$

Where:

M_y is the moment with respect to the y axis.

A is the area of the figure

$\bar{X}$ if the normal distance from the y axis to the centroid of the area A.

If an area is divided into a number of subareas, the moment of the entire area is equal to the sum of the moments of the subareas. In the former notation, this may be stated mathematically as:

$$M_y = A_{T_1} \bar{X}_1 + A_{T_2} \bar{X}_2 + \ldots + A_{T_N} \bar{X}_N \qquad [12]$$

Equating the right-hand sides of equations [11] and [12] and solving for $\bar{X}$:

$$\bar{X} = \frac{A_{T_1} \bar{X}_1 + A_{T_2} X_2 + \ldots + A_{T_N} \bar{X}_N}{A} \qquad [13]$$

The quantity $(A_{T_1} \bar{X}_1)$ is the area of a trapezoid times the normal distance from the Y axis to the centroid of the area, A_{T_1}. The trapezoid again may be considered to consist of a rectangle and triangle. Equations [4] and [5] represent the computations of the areas of the rectangle and triangle, respectively. The sum of the moments of the two portions of the trapezoid would represent the moment of the trapezoid. Inserting the moment arm $(\bar{X}_1)$ for the trapezoid in equations [4] and [5] results in:

$$A_{T_1} \bar{X}_1 = [(y_2-y_1)\, x_1](x_1) + \underset{(2)}{(y_2-y_1)} \frac{(x_2-x_1)}{2} \quad (x_1 + \frac{x_2-x_1}{3}) \qquad [14]$$

Similar solutions can be obtained for the remaining trapezoids. These values can be substituted in equation [13] for $\bar{X}$. The resulting equation can be generalized (as [8] was from [7]) and the following obtained:

$$\bar{X} = \frac{|M_y|}{|A|} = \frac{\left| \sum_{n=1}^{N+1} \left[\Delta y_n \frac{(x_n)^2}{2} + (\Delta y_n) \frac{(\Delta x_n)}{2} \left(x_n + \frac{\Delta x_n}{3}\right) \right] \right|}{|A|} \qquad [15]$$

By similar methods:

$$\bar{Y} = \frac{|M_x|}{|A|} = \frac{\left| \sum_{n=1}^{N+1} \left[\Delta x_n \frac{(y_n)^2}{2} + (\Delta x_n) \frac{(\Delta y_n)}{2} \left(y_n + \frac{\Delta y_n}{3}\right) \right] \right|}{|A|} \qquad [16]$$

Equations [8a] and [15] and [16] were used in computing the area and centroid, respectively, of the radar echoes.

Data Collection Procedure

Film of the radar scope (PPI) at Amarillo, Texas, from May 1, 1961, to September 1, 1961, was used for the study. Operating characteristics of the WSR-57 radar from which the film was obtained are listed in Table I. Certain portions of the film were rendered unusable because of malfunctioning equipment or because the camera was not in operation. Periods of time for which film was usable and unusable are presented in Table II with the primary reasons why the film was not usable. Film for dates other than those shown in Table II was not usable because the time on the film was not readable. Periods when the camera was not in operation usually are periods of little or no rainfall within the area covered by the radar.

Other basic data also came from the U. S. Weather Bureau. These included Radar Reports (RAREPS) from the National Weather Records Center, Ashville, North Carolina, synoptic weather maps, and hourly precipitation data for Texas and New Mexico.

The equipment used for data collection is shown schematically in Figure 7. The 16 mm. film was placed on a projector. Individual frames were then inspected manually or viewed at a wide range of film speeds. Plate glass, 1/4-inch thick, was used for a screen. A map[1] on which the study area was delineated was placed on the back (with respect to the projector) of the screen. Over the study area was placed a transparent plastic overlay on which lines representing 5-mile grids had been drawn. A 20-mile square consisting of 1-mile grids was moved on the map from one location to another when measuring an echo. The 20-mile square was used as a vernier to obtain coordinates to the nearest mile.

---

[1]Lambert Conformal Conic Projection, Standard Parallel at 33°, and a scale of 1:1,374,400.

TABLE I

OPERATING CHARACTERISTICS OF THE WSR-57, U.S. WEATHER BUREAU RADAR, AMARILLO, TEXAS

Peak Power Output	500 kw.
Wave Length	10 cm.
Pulse Length (long)	4 μsec.
Pulse Length (short)	0.5 μsec.
Minimum Detectable Signal	
Long Pulse	103 dbm.[1]
Short Pulse	93 dbm.[1]
Pulse Repetition Frequency	
Long Pulse	164 per sec.
Short Pulse	656 per sec.
Antenna	12' Parabolic bowl
Beam (horizontal and vertical width)	2.2 degrees

[1]Theoretical value

TABLE II

PERIODS OF USABLE AND UNUSABLE RADAR FILM, AMARILLO, TEXAS, 1961

From Day	From Hour	To Day	To Hour	Usable	Not Usable	Remarks
1961		1961				
June 26	0800	June 26	1100		x	Over exposure and time gaps in film
26	1100	27	0718	x		
27	0718	27	1707		x	No record (RAREPS indicated no precipitation in the area)
27	1707	28	0606	x		Two echoes not measured at N. M. line because of no ending time
28	0606	28	1606		x	No record
28	1606	29	0036	x		AP extended south from G. C.
29	0036	30	1652		x	No record (RAREPS indicated one small area of precipitation)
30	1652	30	2158	x		
30	2158	July 1	0200		x	No record (RAREPS did not indicate precipitation in the area)
July 1	0200	1	0518	x		No echoes measured-considerable AP present
1	0518	1	1203		x	No record
1	1203	3	0037	x		1900-2300 line dissipated in the area; 7/1-2200 to 1014 7/2 3 lines in the area; 5 echoes on scope at end
3	0037	3	0800		x	No record
3	0800	3	1948		x	No echoes measured-beginning times were not available on most of echoes so none were measured
3	1948	5	1059		x	No record (RAREPS indicated precipitation in the area on 7/4)
5	1059	6	0152	x		No echoes in area
6	0152	6	1405		x	No record (RAREPS indicated no echoes in area)
6	1405	7	0656	x		No echoes in area
7	0656	8	1621		x	No record
8	1621	9	1953	x		Line in area-no echoes measured
9	1953	10	0310		x	No record
10	0310	10	0348		x	Not long enough record
10	0348	10	1555		x	No record
10	1555	11	0926	x		0600-0800 line in area. Roll of film ended at this time.

TABLE II (Continued)

From Day	From Hour	To Day	To Hour	Usable	Not Usable	Remarks
11	0926	11	2335		x	Break that occurred with change in film roll
11	2335	15	1829	x		Continuous except for occasionally one echo
15	1829	16	0256		x	Time not readable
16	0256	16	0455		x	Film for 100 mile range
16	0455	16	1259		x	No record
16	1259	17	0213	x		
17	0213	17	1633		x	No record
17	1633	17	1758		x	Time undistinguishable
17	1758	18	0106	x		
18	0106	18	1634		x	No record
18	1634	20	0808	x		Remainder of film had undistinguishable time. Roll of film was changed and initial portion of film time was undistinguishable
August		August				
2	2000	3	0455	x		
3	0455	3	1703		x	No record
3	1703	3	2045	x		
3	2045	4	1009		x	Time undistinguishable and no record
4	1009	4	1056	x		
4	1056	5	1759		x	No record
5	1759	5	2343		x	Blank film and undistinguishable time
5	2343	7	1429	x		
7	1429	8	1801		x	No record
8	1801	11	0538	x		Several areas of precipitation classed as lines
11	0538	12	0108		x	Radar operated on 100 mile range and undistinguishable time
12	0108	12	0856	x		Air mass showers-no echoes measured
12	0856	12	1949	x		Numerous convective echoes-film roll ended at 1949.

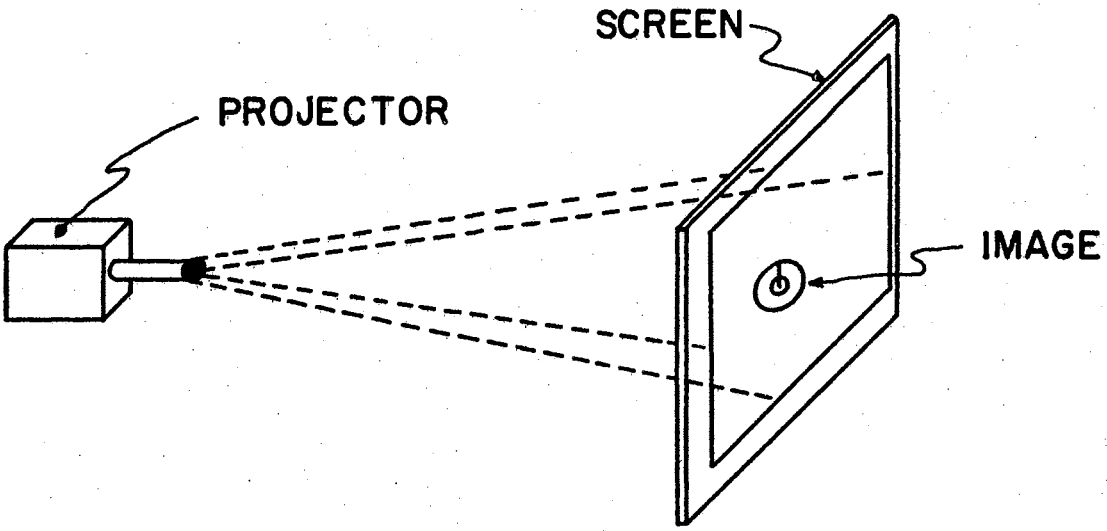

Figure 7. Schematic diagram of the data collection equipment.

Observation procedure: The image projected on the screen was oriented both vertically and horizontally by matching reference points on the screen and frame of film. Desired picture scales were obtained by comparing known distances in the picture to known distances on the screen.

An observation of an echo consisted of noting the time, tendency, and towns over which it had occurred and obtaining x,y coordinate readings on the periphery. The distance separating the readings around the echo was determined by approximating the periphery by a series of straight lines. The x,y coordinate readings were taken frequently enough to obtain the area over which the echo was present. Figure 8 presents a sample echo as it would appear on a portion of the screen. The circles correspond to points where x,y coordinates were obtained. The data input and output of the computer for the echo (No. 12) are presented in appendices A and B.

To obtain consistent data throughout the collection period, certain rules were established for specified situations. The following situations were handled by specific rules.

Three criteria were used in determining the frequency with which measurements were made. These were: (1) speed, (2) initiation and dissipation points, and (3) changes in shape, area, and tendency[2]. Frequent readings were taken on fast-traveling echoes. This gave more accurate speed and direction variations during their life cycle. Readings were also obtained at the points of echo initiation and dissipation to show total distance traveled. As appreciable changes in shape, area and tendency occurred, readings were obtained. The ending time used in computing echo duration was that time when it could no longer be seen on the scope.

---

[2]Tendency as used by the writer indicates strength or brightness of the echo image on the PPI scope.

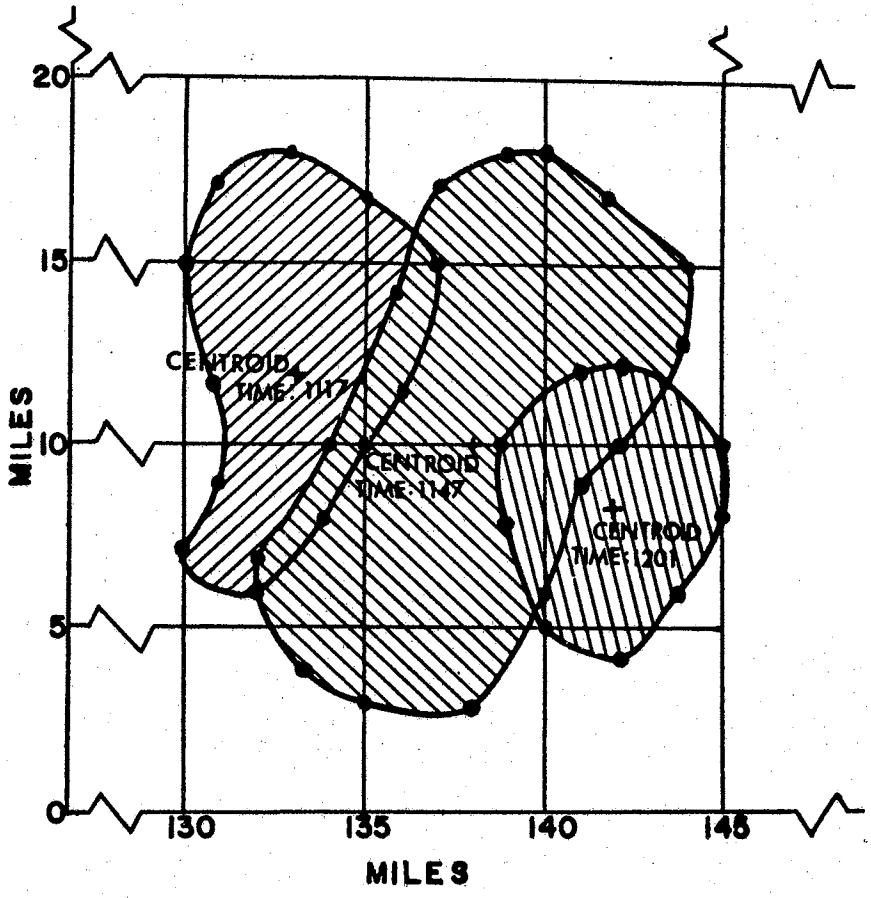

Figure 8. Schematic diagram of echo No. 12 (July 13, 1961) at three different times during its life cycle. The circles correspond to points where x,y coordinate values were obtained.

All the towns over which the echo occurred were listed. This was done to compare the occurrence of rainfall at the U. S. Weather Bureau rain gages within the study area with the occurrence of an echo over a particular locality. This was used to test the validity of the assumption that the radar echo represented actual precipitation on the ground.

Merging and separating echoes: Merging and separating echoes were measured as consistently as possible. If one echo separated into two distinct parts, the echoes after separation were given two new numbers. However, if no erroneous travel distance resulted, one of the parts retained the original number. Merging echoes were handled in a similar manner. As long as the outlines of the merging echoes could be determined, the two echoes were recorded as separated.

Separating and merging echoes give erroneous values for speed and distance traveled when computed using the centroid of the echo. The values are erroneous because the changes are not entirely due to movement of all points on the echo an equal distance per unit of time. The values for movement are partially due to an increase in echo size in one direction which results in the centroid moving in that direction. Thus, translation and propagation are combined in the movement.

Echoes included in study: Echoes were included in the study only when an ending and beginning time were available. (For purposes of this study, the time echoes entered or left the area was also considered to be their beginning or ending times, respectively.) For example, the period of record on July 3, 1961 (see Table II) was eliminated because numerous echoes had developed before the film record started. These were eliminated because there were no beginning times available.

Echoes originating or moving outside the study area: Echoes originating outside and moving into the area and those originating in the area and moving outside were studied using the following procedure. When an echo entered the area the time was noted and an observation obtained, provided most of it was within the area. Thus, a representation of the echo configuration was obtained. If the echo was moving slowly with only a small fraction in the area, no observation was obtained; however, a notation of the time was made.

Delineation of line: To be classified as a line one echo or group of echoes must have: (1) Rectilinear appearance, aligned along an approximate straight line with a length of 50 miles or more and, in addition, for a group of echoes, four had to be present at a minimum distance of 50 miles with not more than 10 miles between any two; and (2) sharply defined outlines, especially on the leading edge. To be measured, an echo could not have been part of a line during its life cycle. Thus, echoes were studied before they moved into the area and after they moved out to determine if at any time they would have been classified as a line. Figure 9 shows the early stage of several echoes that would not be classified as a line. However, in less than two hours they had developed into a line as shown in Figure 10.

Determination of ground clutter: Ground clutter as used in this thesis is defined as that return immediately around the radar site that is normally a part of the return on a PPI scope. Ground clutter is identified in Figures 9 and 10. One of the reasons for the selection of the study area was that ground clutter would not normally interfere with the measurement of precipitation echoes. However, on several occasions it did expand and extend into the study area. Normally, when precipitation was occurring, ground clutter was not present within the area.

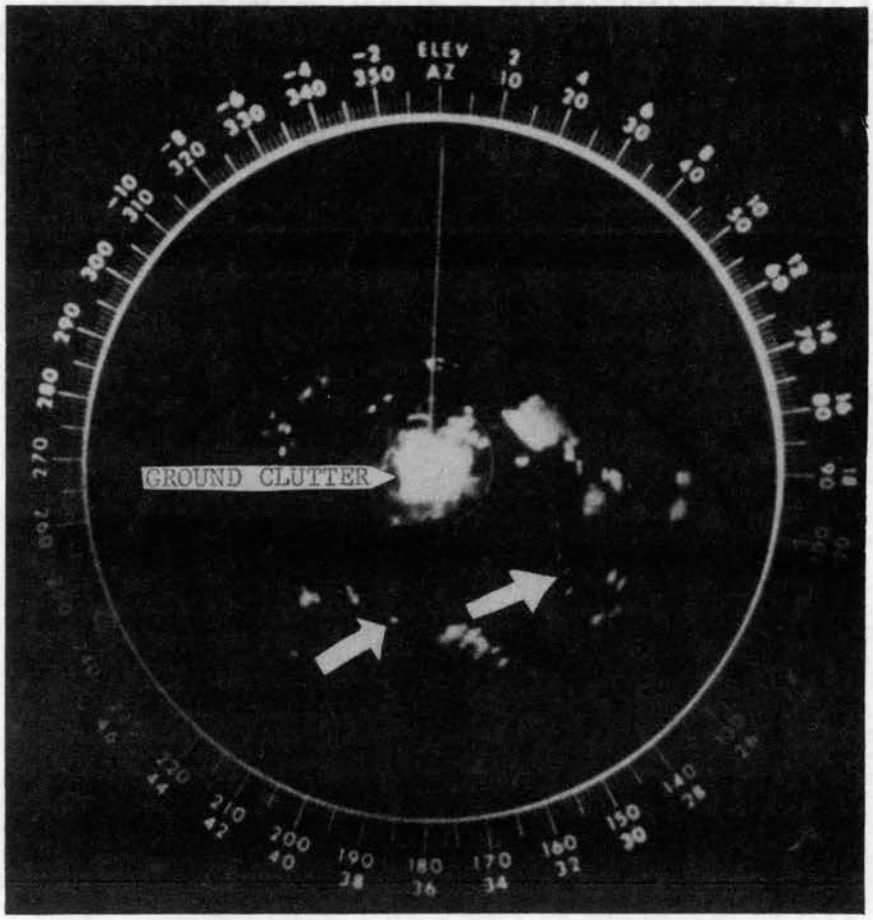

Figure 9. Early stage of a line on July 2, 1961 at 1541 in which echoes appear randomly arranged. (Arrows point to random echoes).

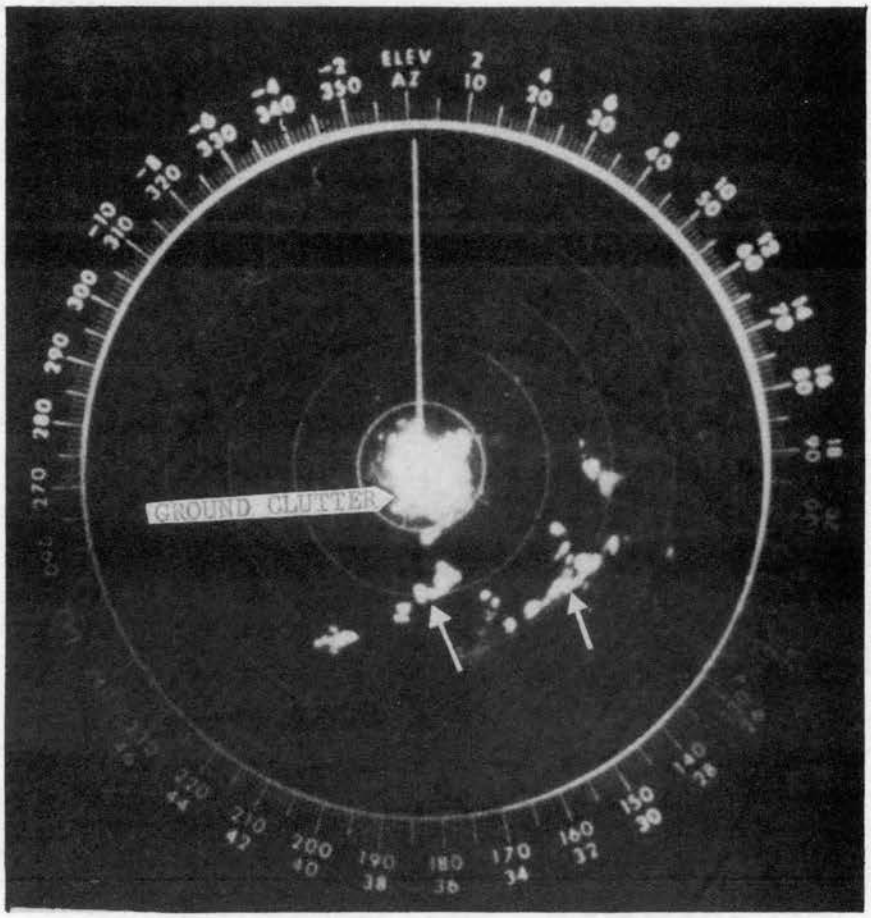

Figure 10. Development of early stage of line shown in Figure 9 into a line at 1720, July 2, 1961, (Arrows point to lines).

Abnormally large ground clutter patterns were observed when weather was detected at long ranges. As the weather moved in toward the radar station, the ground clutter pattern shrank to its normal size. Hiser and Freseman (21) observed the same phenomena and attributed it to super-refraction of the radar beam resulting from stable atmospheric conditions. The weather destroys the stability and the ground clutter shrinks to a normal size.

Anomalous propagation (AP): A detailed discussion of the phenomena of anomalous propagation is beyond the scope of this thesis, but detailed discussions have been presented many times; e.g. Battan (2) and Hiser and Freseman. (21). AP is defined in this thesis as the detection of ground targets at abnormal ranges. It is produced by abnormal bending of the electromagnetic waves propagated by the radar. The waves strike the ground at great ranges, and the return is presented on the PPI scope. Temperature inversions, steep moisture lapses, or a combination of both form ducts that trap the waves and produce the abnormal bending. The conditions whereby the ducts may be formed are not usually present when precipitation is in the area. Thus, the presence of AP and precipitation echoes within the same area on the scope does not occur frequently. However, occasionally both may occur during the decaying stages of a thunderstorm.

RAREPS, prepared by the radar operator, and rainfall records were used as aids to identify precipitation echoes from AP. An example of the type of AP that occurred during this study is presented in Figure 11. This was judged to be AP because: (1) no precipitation was measured in that area, (2) the area was not listed in the RAREPS as prepared by the radar operator, and (3) the size of the return fluctuated rapidly from frame to frame.

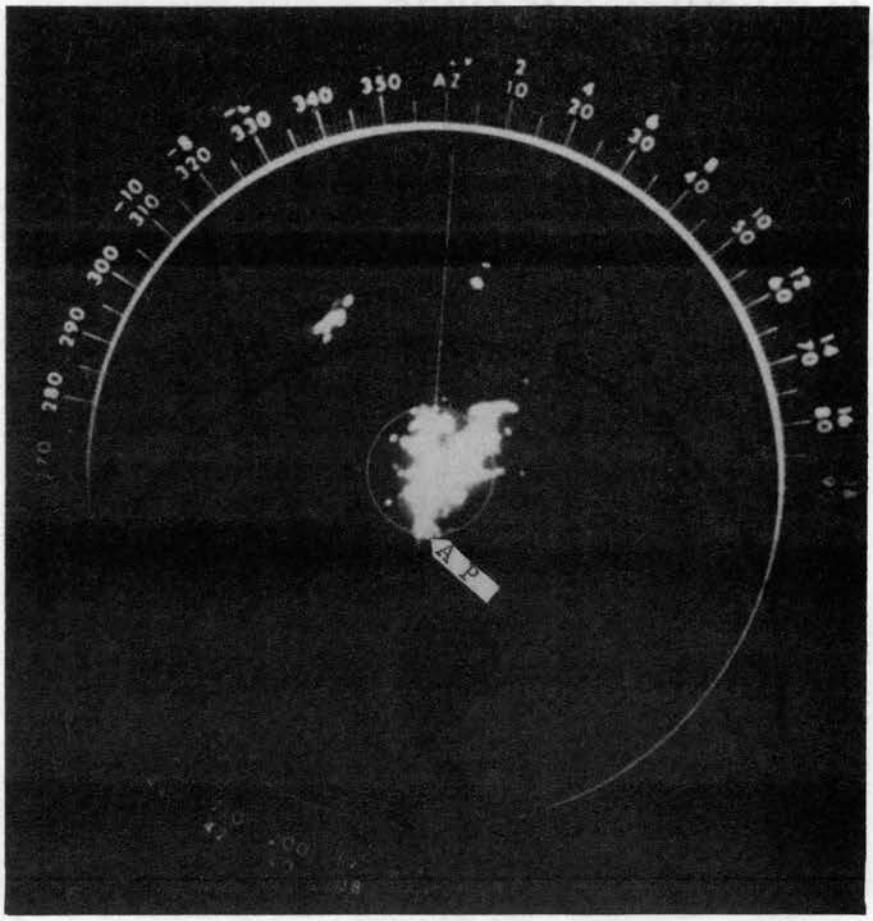

Figure 11. Typical anomalous propagation encountered in this study, June 28, 1961 at 2126. (Arrow points to portion of the return that is AP).

False echoes: Another return frequently seen on the radar scope was apparently caused by the Amarillo Airport control tower. The false echoes occurred to the southeast of the radar. When precipitation occurs to the northwest of the radar, a portion of the signal that returns to the antenna travels past the antenna and strikes the control tower. This is in turn reflected to the antenna by the tower. The signal may be bounced back and forth from the tower to the precipitation echo and back so that a sweep trace may present several echoes at varying ranges in an elongated, radial pattern from the radar site. An example of the false echoes that occurred during this study is presented in Figure 12.

Because of the magnification of the film, aircraft produced returns that ranged from 3 to 5 miles in diameter. These echoes were distinguishable as aircraft because thay were less than 5 miles in diameter, had durations usually less than 9 minutes, and traveled at the rate of 3 to 5 miles per minute. Therefore, echoes of this type were eliminated from consideration.

In summary, some of the criteria used to determine whether a particular radar echo was a precipitation echo or some other type of return were: (1) Was the speed of the echo excessive? (2) Did the echo occur over a town so that it could easily be the return from a grain elevator? (3) Was the rate of change or fluctuation of the echo area on the scope excessive? (4) Did the echo move during its life cycle? (5) Was there any precipitation recorded for any of the towns which the echo was over during its life cycle? These procedures did not guarantee that all echoes measured during this study were from precipitation but did tend to limit the number of non-precipitation ones included in the study.

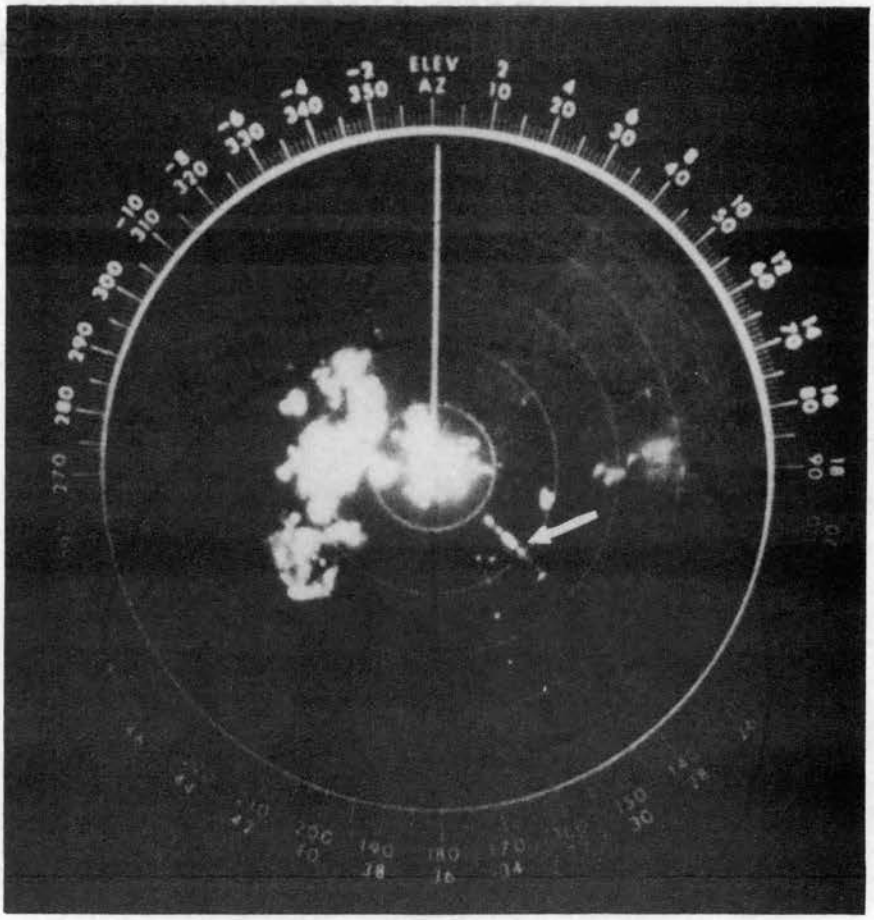

Figure 12. Typical false echoes caused by airport control tower that occured in this study, July 14, 1961 at 0012. (Arrow points to the radially projecting echoes caused by tower).

Data Analysis Procedure

The data obtained for radar echoes were punched on cards for analysis by a high speed computer. Each card contained an echo number, time of echo occurrence, data that identified the card to facilitate computer computations, and x or y coordinate values for that observation.

An IBM 709 computer was programmed[3] to make the following computations:

(a) Area, A

(b) Centroid, $\overline{X}$, $\overline{Y}$

(c) Time interval between successive readings

(d) Distance traveled between successive readings

(e) Direction toward which echo travels between successive readings--defined as an azimuth from 0 to 360 degrees in a counter-clockwise direction with north as 0

(f) Average speed between successive readings

(g) Total duration

(h) Total distance traveled

(i) Resultant direction toward which echo travels as determined by the initiating and ending points of the echo--defined as an azimuth from 0 to 360 degrees in a counter-clockwise direction with north as 0

(j) Average speed of the echo--determined by a ratio of the total distance traveled to total duration

Appendices A and B may be consulted for samples of data input and output, respectively, for the computer.

---

[3]Programmed by Glen N. Williams, Data Processing Center, Texas Engineering Experiment Station, College Station, Texas.

A duration weighted, average echo area was computed in the following manner:

$$A_m = \frac{\frac{1}{2}\sum_{i=1}^{n}(a_i+a_{i+1})\ (t_{i+1} - t_i)}{(t_{n+1} - t_1)}\ , \quad \text{and } a_n = a_{n+1} \qquad [17]$$

A_m is the duration weighted, average echo area

a is the echo area determined at time, t

i = 1, 2, 3, ..., n. indicates sequential values of area and time.

Frequency distributions of the data were then made to indicate the variation of echo characteristics.

CHAPTER V

RESULTS

Limitations and Completeness of Data

The results presented for this study have certain limitations. These are results from one year, 1961, and for specified intervals of time that are intermittent. Thus, the characteristics of radar echoes presented here represent charzcteristics for portions of 1961 only.

Table III gives a classification of echoes for this study. Most of the data presented are for only those echoes which stayed in the study area from initiation through dissipation. Approximately 52 percent of the echoes assigned numbers were in this class and had complete data for their life cycle. Forty-two of the numbers assigned were assigned to combined or split echoes (Table III) and formerly carried a different number. Thus, in reality, 64.4 percent of the total number of echoes had complete data. The primary reason for the lack of complete data for an echo was that the echo initiated outside the area. Merging or separating of the echoes was the next reason for lack of complete data.

To evaluate the reliability of radar echoes representing measureable rainfall at the ground surface, attempts were made to relate rainfall to the presence of an echo over a rain gage. The results obtained are presented in Table IV. Forty-two times echoes occurred

TABLE III

CLASSIFICATION OF ECHOES FOR THIS STUDY

Class Code	Class Description	Number	Percent of Total
Complete	Data for complete life cycle available	171	51.7
IA	Came into area after initiation	49	14.8
OA	Passed out of area after initiation	20	6.0
Separated	Separated into two or more echoes	5	1.5
Joined	Joined, or was joined by, another echo	38	11.5
Fmly	Formerly another echo number. New number assigned because it Broke Up or was Joined	42	12.7
Omit	Omitted for various reasons	6	1.8
	Total:	331	100.0

over rain gages and 10 times rain was recorded. Thus rainfall was recorded at a rain gage approximately 25 percent of the time that the radar showed an echo over a gage. Of the 32 times no rain was recorded, 8 times the gage was under the edge of the echo and 7 times the echo was initiating or dissipating when over the gage. The absence of measured rainfall was at least partially due to the following factors:

1. The lack of continuous coverage with time of the radar film.
2. Detailed accounting of precipitation from echoes classed as "lines" was not made.

TABLE IV

COMPARISON OF THE NUMBER OF ECHOES OCCURRING OVER RAIN GAGES WITH THE NUMBER OF RECORDED RAINFALL EVENTS

Number of echoes occurring over rain gages	42
Number of times rain recorded	10
Number of times gage on the edge of echo	8
Number of times echo initiating or dissipating when over the gage	7

Meteorological factors which may have contributed to the absence of measured rainfall when an echo was present over a rain gage were:

1. Wind shear causing the rain to fall on an area other than the area over which the radar depicted the echo.
2. Virga which results in the evaporation of rain drops before they reach the ground.

3. Speed of droplet fall which results in a time lapse between the time the radar beam intercepts rain drops at a particular elevation and the time the drops reach the ground.

Factors related to radar operating characteristics were:

1. Distortion of the radar echo from its true shape due to the effects of the pulse length and beam width.
2. Earth curvature effects on the location of the echo by radar and the true location of the rainfall area.
3. Effect of range on radar echo representation.

The writer believes that the poor comparisons between the presence of an echo over a rain gage and measured rainfall were more related to the limitations of procedure used than to poor reliability of the radar depicting actual rainfall.

Evaluation of Area and Centroid by Coordinates

A method was developed whereby radar echoes depicted on the PPI scope were converted to digital form by a sequence of x,y coordinates obtained around the periphery of the echo. These data were then placed on punch cards and summarized by a high-speed computer. Further mechanization of the data collection process may be accomplished by utilizing an analogue to digital converter.

The accuracy of the coordinate method for computing areas and centroids is determined by the precision with which the echo periphery is defined as a sequence of straight lines. Thus, any degree of accuracy can be obtained. Areas determined by the coordinate method deviate less than 5 percent from those obtained by planimetering. In general, these errors are conservative; i.e., the area computed by the coordinate method will be slightly less than the actual echo area.

Duration, Distance, Speed, and Direction

Figure 13 presents a frequency distribution of echo durations for which complete data were available. The frequency distribution is different from the conventional in that it has unequal duration intervals. The short intervals of 0.1 hour from 0 to 0.6 hour were used to show in detail how a large number of the echoes varied in duration. The interval was changed for the longer duration intervals for the following reasons:

1. For the longer durations, whether the echo lasts 1.5 or 1.6 hours makes little difference.
2. Due to the small size of the sample, anomalies would occur in which several short intervals would be zero and one would present a small peak.

Thus, each interval was reduced to an equivalent number per 0.1 hour interval; e.g. for the 0.6 to 0.8 hour interval the total number that occurred was divided by 2 as this interval was twice the 0.1 hour interval.

Median duration of the radar echoes of convective precipitation was 0.6 to 0.8 hour and the mode was 0.2 to 0.3 hour. Figure 14 and Table V show that 80 percent of the echoes had durations of less than or equal to 1.5 hours.

Distance traveled by each echo for which complete data were available is shown in Figure 15 and Table VI. Most frequently the echoes were stationary and the median distance traveled was between 0 and 5 miles. These movement characteristics are intermediate between results obtained in Arizona and South Texas. In studies of convective precipitation in Arizona (19) all echoes traveled less than 6 miles.

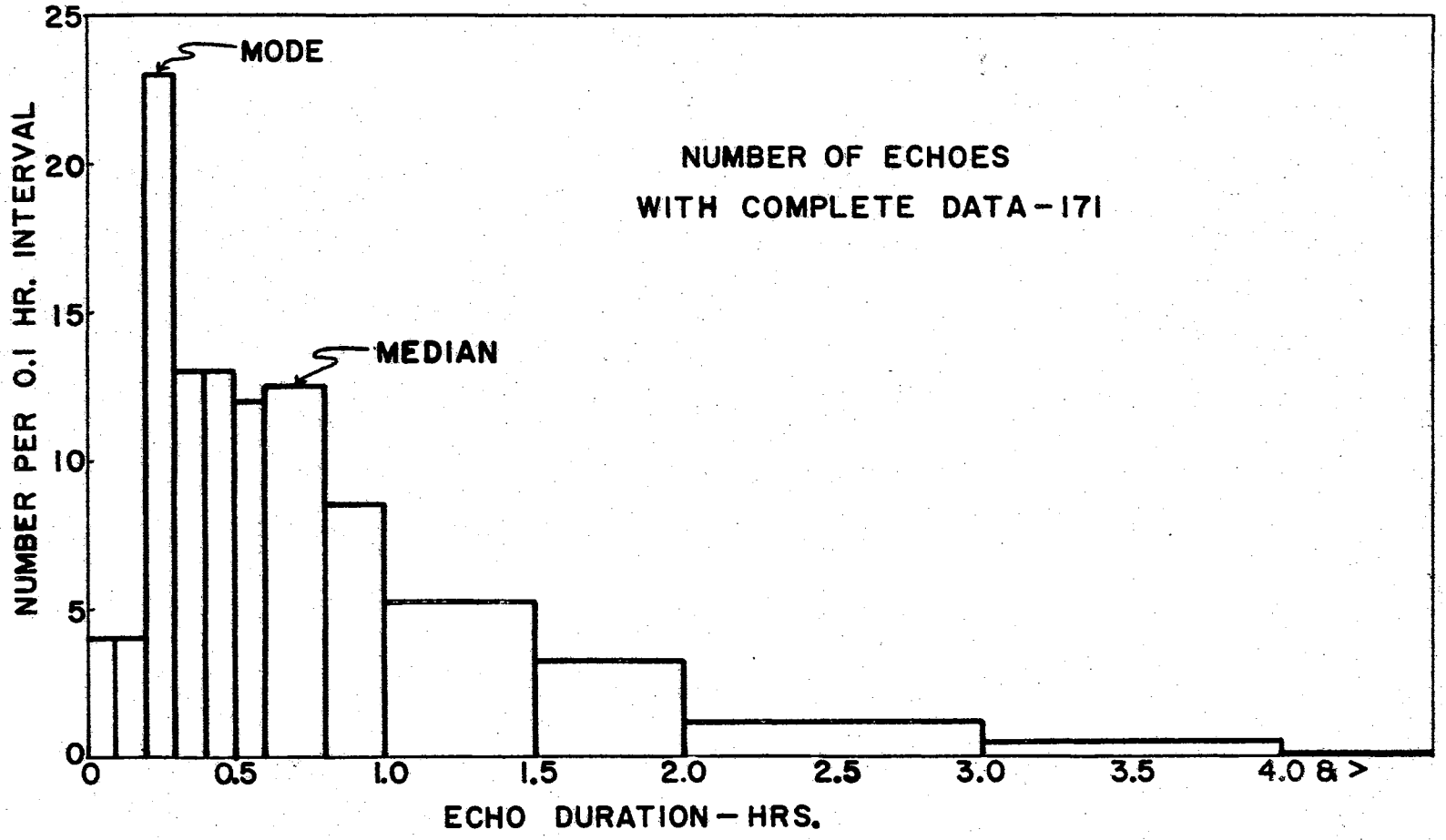

Figure 13. Frequency distribution of durations for indicated intervals of duration.

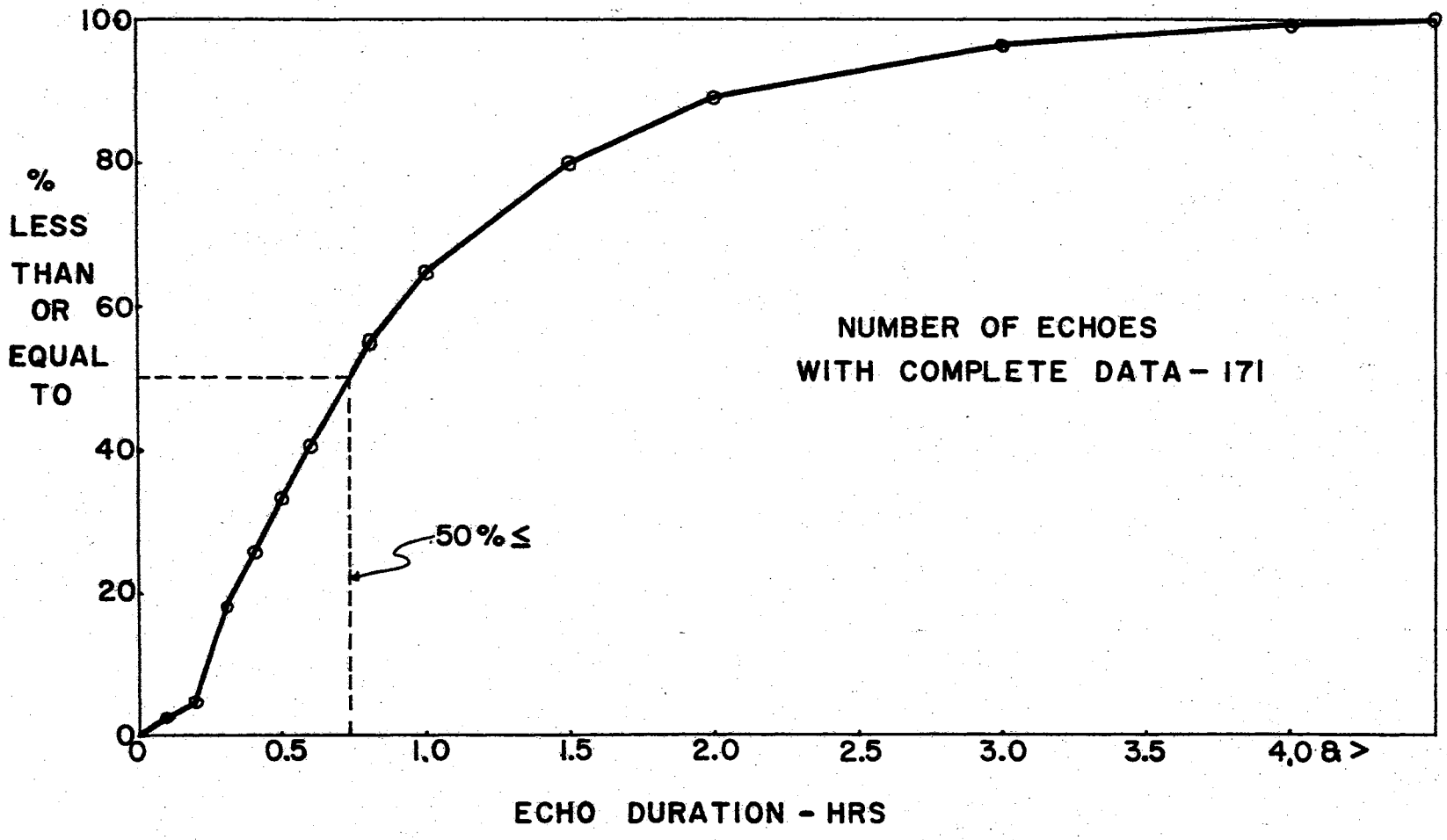

Figure 14. Cumulative percent of total number less than or equal to indicated duration.

TABLE V

DURATION OF ECHOES WITH COMPLETE DATA AND FOR INDICATED INTERVALS

Interval (Hours)	Number	Accum.	Percent of Total Number Accum.	Number Per 0.1 Hour Interval
$> 0 \leq 0.1$	4	4	2.3	4
$> 0.1 \leq 0.2$	4	8	4.6	4
$> 0.2 \leq 0.3$	23	31	18.1	23
$> 0.3 \leq 0.4$	13	44	25.7	13
$> 0.4 \leq 0.5$	13	57	33.3	13
$> 0.5 \leq 0.6$	12	69	40.3	12
$> 0.6 \leq 0.8$	25	94	54.9	12.5
$> 0.8 \leq 1.0$	17	111	64.8	8.5
$> 1.0 \leq 1.5$	26	137	80.0	5.2
$> 1.5 \leq 2.0$	16	153	89.4	3.2
$> 2.0 \leq 3.0$	12	165	96.4	1.2
$> 3.0 \leq 4.0$	5	170	99.3	0.5
> 4.0	1	171	99.9	0.1

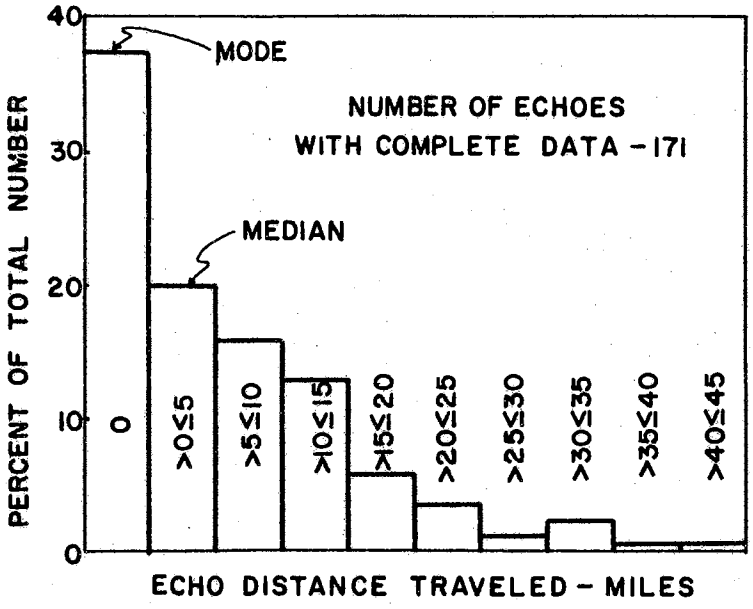

Figure 15. Frequency distribution of distances traveled for indicated intervals of distance.

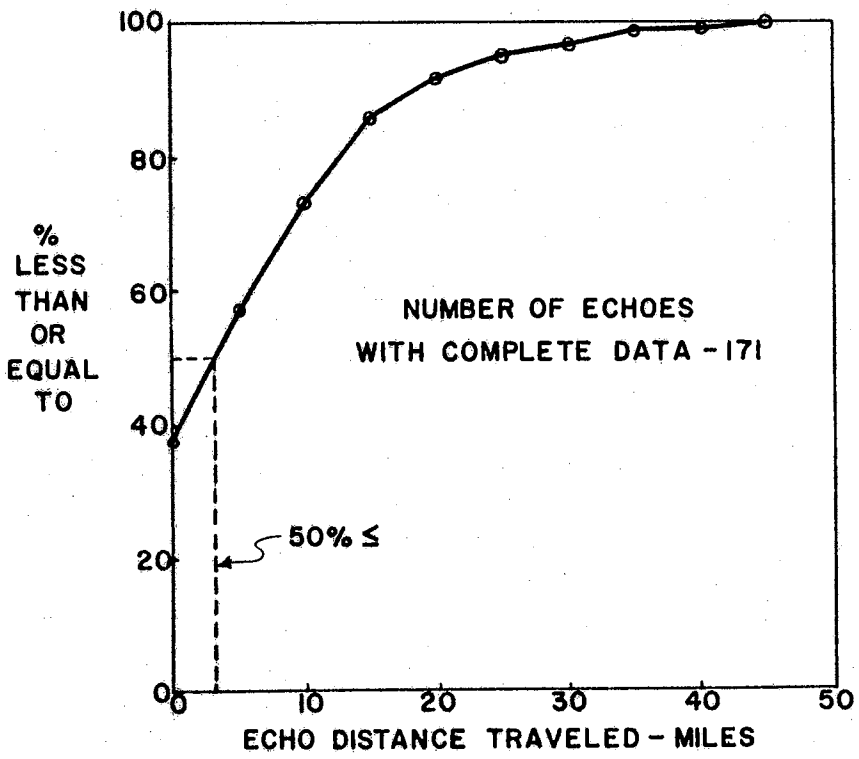

Figure 16. Cumulative percent of total number less than or equal to indicated distance traveled.

TABLE VI

DISTANCES TRAVELED BY ECHOES WITH COMPLETE DATA AND FOR INDICATED INTERVALS

Interval (Miles)	Number	Accum.	Percent of Total Number	Accum.
0	64	64	37.4	37.4
$> 0 \leq 5$	34	98	19.9	57.3
$> 5 \leq 10$	27	125	15.8	73.1
$> 10 \leq 15$	22	147	12.9	86.0
$> 15 \leq 20$	10	157	5.8	91.8
$> 20 \leq 25$	6	163	3.5	95.3
$> 25 \leq 30$	2	165	1.2	96.5
$> 30 \leq 35$	4	169	2.3	98.8
$> 35 \leq 40$	1	170	0.6	99.4
$> 40 \leq 45$	1	171	0.6	100.0

Most of the echoes studied by Clark (13) in South Texas had greater movement. The High Plains is geographically intermediate between these areas and could be expected to have intermediate meteorological characteristics.

Sixty percent of the echoes studied traveled less than or equal to six miles (Figure 16) while 92 percent traveled less than or equal to 20 miles. These relatively short distances traveled decreases the total area covered by any one storm, but increases the possibilities that one watershed will receive runoff-producing rainfall. The smaller the area covered by the cell the greater the volume per unit area of rainfall. The greater the volume per unit area of rainfall the more likely runoff will occur.

The frequency distribution of average echo speed (Figure 17) is similar to the distribution of distances traveled. The mode was no movement, and the median speed was 0 to 5 miles per hour (mph). Ninety-six percent of the echoes had an average speed of less than or equal to 20 mph (Figure 18). Table VII presents the data for the frequency and cumulative distributions of echo speeds.

Direction of movement of radar echoes of convective precipitation (Figure 19) shows two prevailing directions of movement. Thirty-seven percent of the echoes had no movement, but of those that did move, north and south were the two directions most frequently traveled. No dominant direction of movement was indicated.

Preliminary studies by the writer of U. S. Weather Bureau synoptic weather maps for the period during this study indicated upper winds were predominantly to the northeast. Results by Byers and Braham (20) and Ackerman (19) indicated echoes travel in the direction of the mean wind

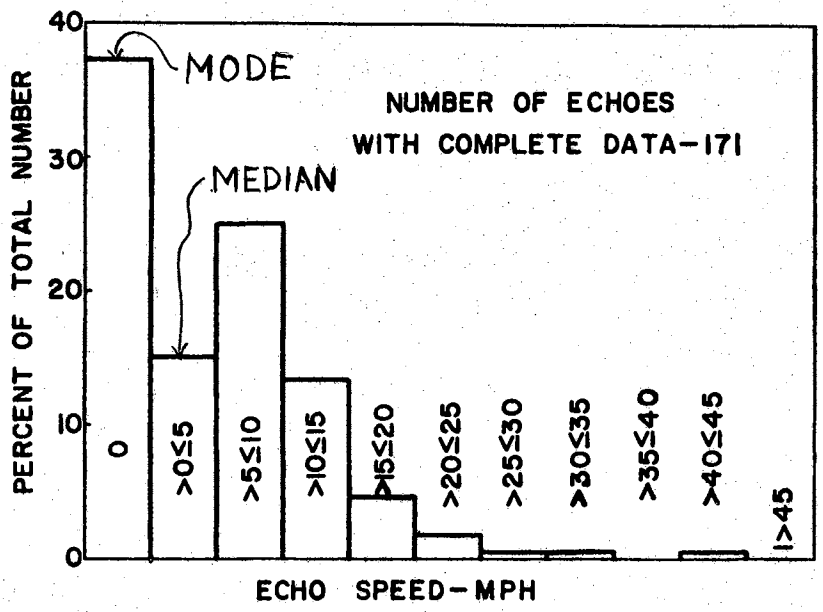

Figure 17. Frequency distribution of echo speeds for indicated intervals of speed.

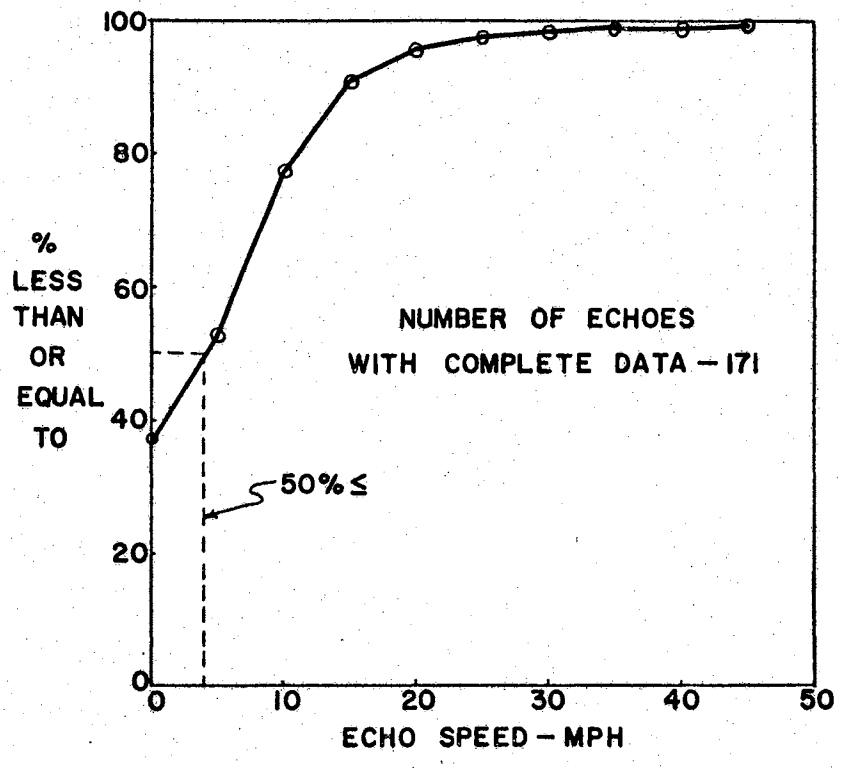

Figure 18. Cumulative percent of total number less than or equal to indicated speed.

TABLE VII

SPEEDS OF ECHOES WITH COMPLETE DATA AND FOR INDICATED INTERVALS

Interval (MPH)	Number	Accum.	Percent of Total	Accum.
0	64	64	37.4	37.4
$> 0 \leq 5$	26	90	15.2	52.6
$> 5 \leq 10$	43	133	25.1	77.7
$> 10 \leq 15$	23	156	13.4	91.1
$> 15 \leq 20$	8	164	4.7	95.8
$> 20 \leq 25$	3	167	1.8	97.6
$> 25 \leq 30$	1	168	0.6	98.2
$> 30 \leq 35$	1	169	0.6	98.8
$> 35 \leq 40$	0	169	0	98.8
$> 40 \leq 45$	1	170	0.6	99.4
$> 45 \leq 50$	0	170	0	99.4
$> 50 \leq 55$	0	170	0	99.4
$> 55 \leq 60$	0	170	0	99.4
$> 60 \leq 70$	0	170	0	99.4
$> 70 \leq 80$	0	170	0	99.4
$> 80 \leq 90$	1	171	0.6	100.0

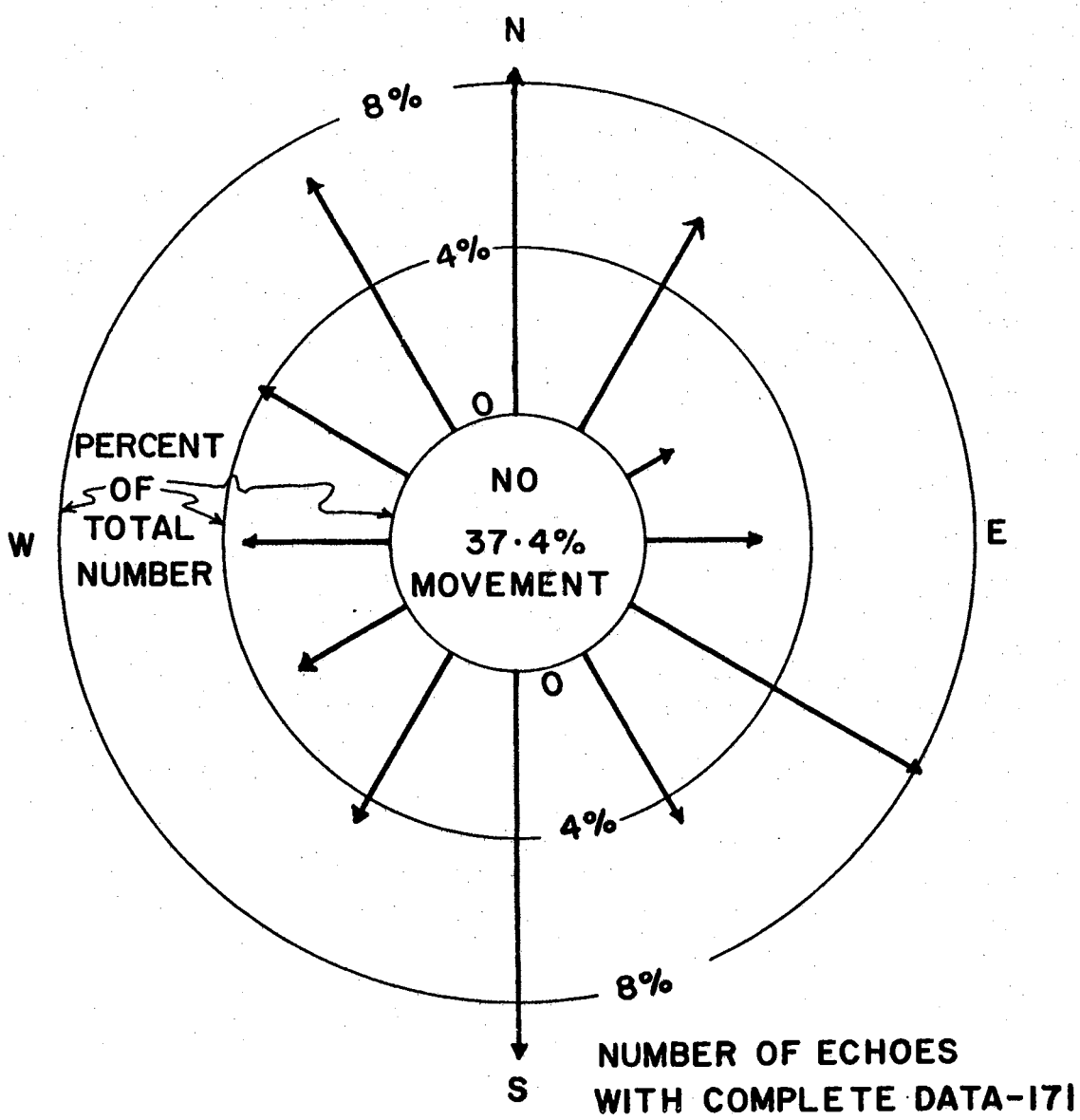

Figure 19. Distribution of resultant directions of movement of echoes by 30 degree intervals and directions indicated.

between the cloud base and top. The data presented in Figure 19 and Table VIII do not indicate this to be true for the High Plains of Texas. One possible explanation is that the echoes occurring in the area are usually associated with frontal passage. That is, they are prefrontal or post-frontal because continental circulation patterns are usually conducive to moisture influx to the area when fronts traverse the area. Study of consecutive upper air maps (500mb) by the writer for the period covered by this study indicated that upper winds usually underwent a 360 degree rotation in direction at intervals of one to seven or more days while fronts approached, entered, and passed through the study area. The direction traveled by the echoes would change as the winds changed. This would then explain the lack of a dominant direction of travel for the echoes.

Time and Location of Initiation

A diurnal distribution of initiation times of all echoes for which the beginning times were available (Figure 20) and Table IX indicated two dominant periods of initiation. This may be more readily seen in Figure 21. The data plotted is a four hour moving average of echoes initiating in the indicated hour. The given hour and the three hours previous were used in computing the average. The dominant periods were shortly after noon and lasting most of the afternoon, and in the evening lasting until 3:00 a.m. The most prevalent period of initiation was centered around midnight (Figure 21).

The afternoon peak in activity is explainable as the normal period in the diurnal cycle when convective activity would be most prevalent. The afternoon is the period of greatest heating, and the initiation process depends on localized heating.

TABLE VIII

DIRECTION OF MOVEMENT FOR ECHOES WITH COMPLETE DATA AND FOR INDICATED INTERVALS

Interval[1] (Degrees)	Number	Accum.	Percent of Total Number	Accum.
> 345 ≤ 015	14	14	8.2	8.2
> 015 ≤ 045	12	26	7.0	15.2
> 045 ≤ 075	7	33	4.1	19.3
> 075 ≤ 105	6	39	3.5	22.8
> 105 ≤ 135	5	44	2.9	25.7
> 135 ≤ 165	8	52	4.7	30.4
> 165 ≤ 195	16	68	9.3	39.7
> 195 ≤ 225	8	76	4.7	44.4
> 225 ≤ 255	14	90	8.2	52.6
> 255 ≤ 285	5	95	2.9	55.5
> 285 ≤ 315	2	97	1.2	56.7
> 315 ≤ 345	10	107	5.8	62.5
No Movement	64	171	37.4	99.9

[1]North is zero and the degrees are 0 to 360 in a counter-clockwise direction.

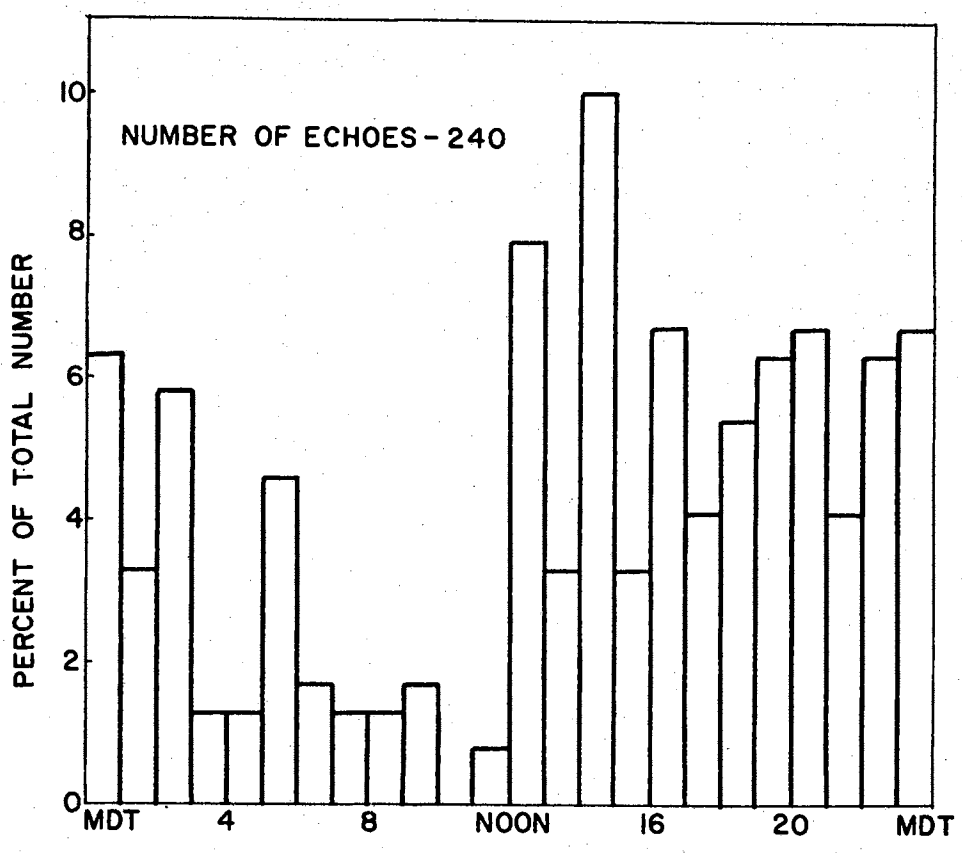

Figure 20. Diurnal distribution of initiating times for all echoes initiating in the study area.

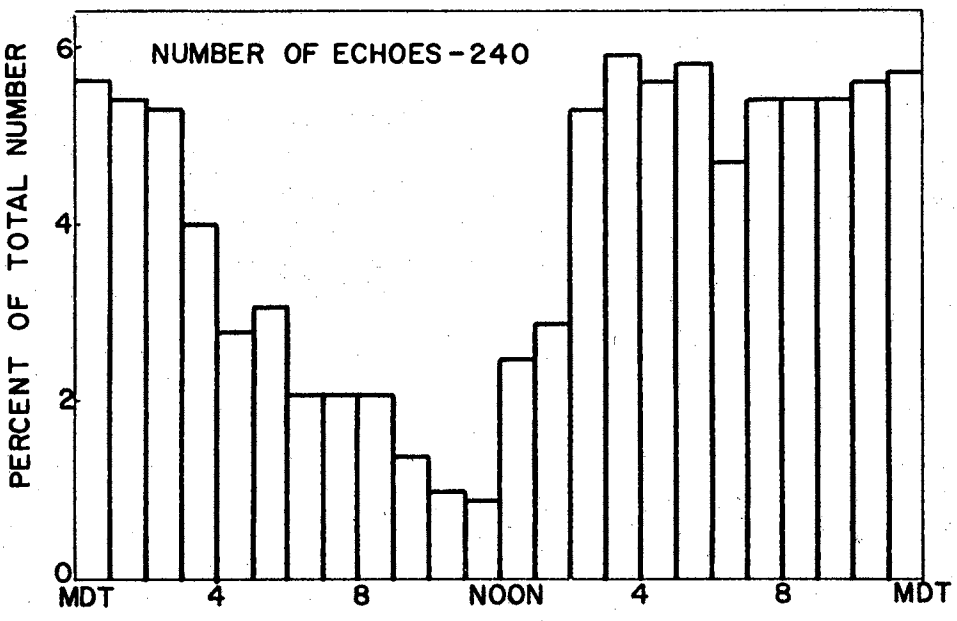

Figure 21. Four hour moving average of diurnal initiating times.

TABLE IX

BEGINNING TIMES FOR ECHOES THAT BEGAN IN THE AREA

Interval (Hours)	Number	Accum.	Percent of Total Number	Four Hour Moving Average Number	Four Hour Moving Average Percent of Total Number
0001 - 0100[1]	15	15	6.3	14.00	5.8
0101 - 0200	8	23	3.3	13.50	5.6
0201 - 0300	14	37	5.8	13.25	5.5
0301 - 0400	3	40	1.3	10.00	4.2
0401 - 0500	3	43	1.3	7.00	2.9
0501 - 0600	11	54	4.6	7.75	3.2
0601 - 0700	4	58	1.7	5.25	2.2
0701 - 0800	3	61	1.3	5.25	2.2
0801 - 0900	3	64	1.3	5.25	2.2
0901 - 1000	4	68	1.7	3.50	1.5
1001 - 1100	0	68	0	2.50	1.0
1101 - 1200	2	70	0.8	2.25	0.9
1201 - 1300	19	89	7.9	6.25	2.6
1301 - 1400	8	97	3.3	7.25	3.0
1401 - 1500	24	121	10.0	13.25	5.5
1501 - 1600	8	129	3.3	14.75	6.1
1601 - 1700	16	145	6.7	14.00	5.8
1701 - 1800	10	155	4.1	14.50	6.0
1801 - 1900	13	168	5.4	11.75	4.9
1901 - 2000	15	183	6.3	13.50	5.6
2001 - 2100	16	199	6.7	13.50	5.6
2101 - 2200	10	209	4.1	13.50	5.6
2201 - 2300	15	224	6.3	14.00	5.8
2301 - 2400	16	240	6.7	14.25	5.9
			100.5	240.00	99.6

[1]0000 is midnight.

Nighttime activity cannot be explained on this basis as there is no localized heating to initiate the convection process. Byers (22) has explained the phenomena of nighttime thunderstorms in the following manner.

> In large areas of the middle western United States thunderstorms occur predominantly at night. These are not to be confused with evening thunderstorms left over from the daytime convection; in fact, they show a peak of occurrence between midnight and 4:00 a.m. Studies have shown that they are caused by a diurnal variation in the large-scale wind system over the continent which is favorable for producing convergence in the low levels in the regions concerned at night.

Byers further concluded that these nighttime thunderstorms have very nearly the same precipitation patterns as those occurring during the daytime. The data presented in Figure 21 agree well with the above explanation as the peak occurs near midnight, and the High Plains is geographically located in the middle western United States.

Locations of initiation for all echoes that began in the area are shown in Figure 22. Three areas of dominant echo occurrence are shown. Several areas over which no echoes initiated are also indicated.

Of the three areas of dominant echo occurrence, two correspond to the northwestern and southeastern edges of the escarpment. The escarpment appears to furnish enough lifting in addition to that present in convection to consistently cause echoes to initiate adjacent to it.

Figures 23 through 26 show the areas of prevalent echo initiation for four different periods of time during the study period. These figures illustrate how the prevalent areas of initiation vary from one period of convective activity to another. The prevalent areas for the four periods (Figures 23-26) differ from the three dominant areas for the complete study period (Figure 22). The dominant areas for the complete

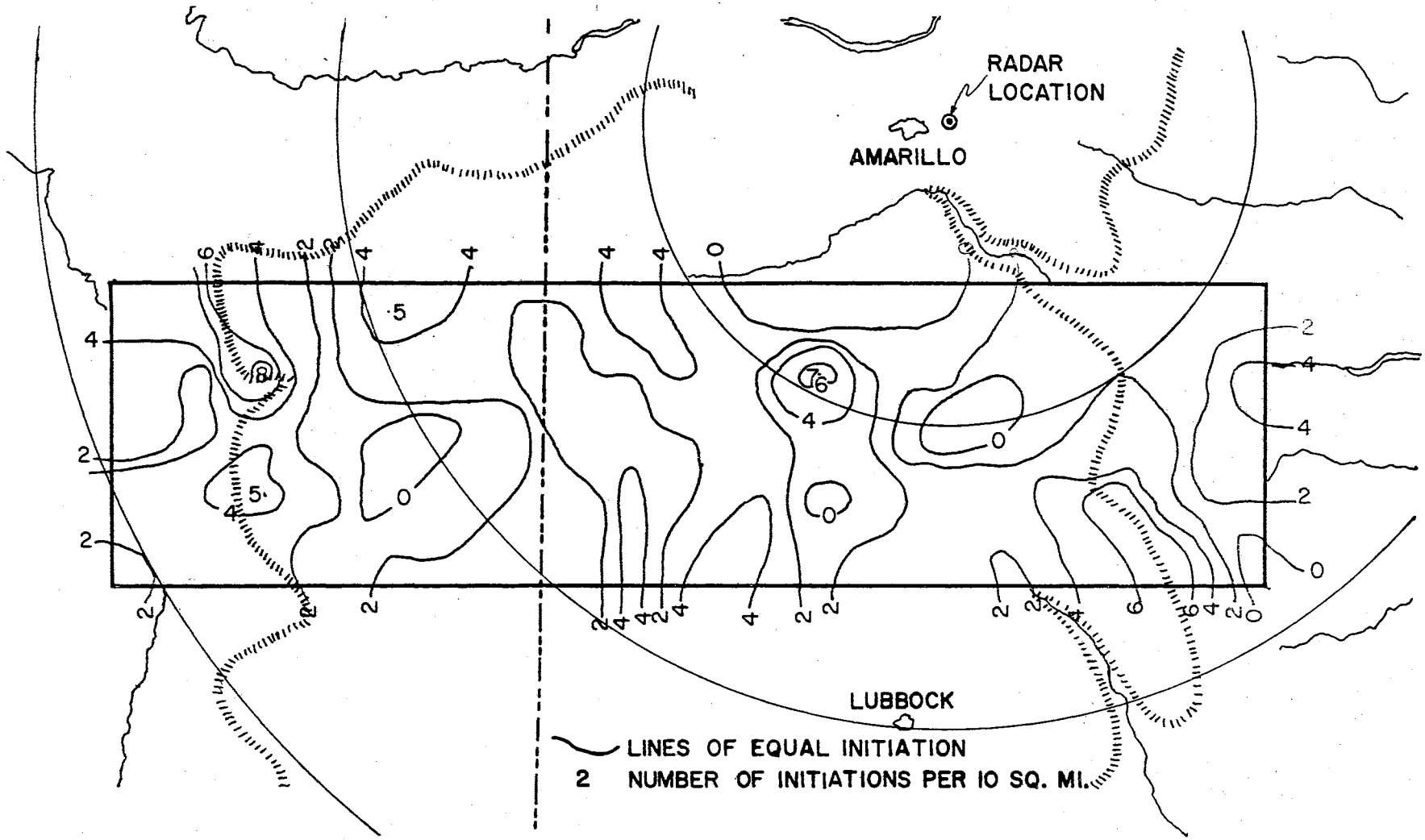

Figure 22. Distribution of locations of initiation for all echoes initiating in the study area.

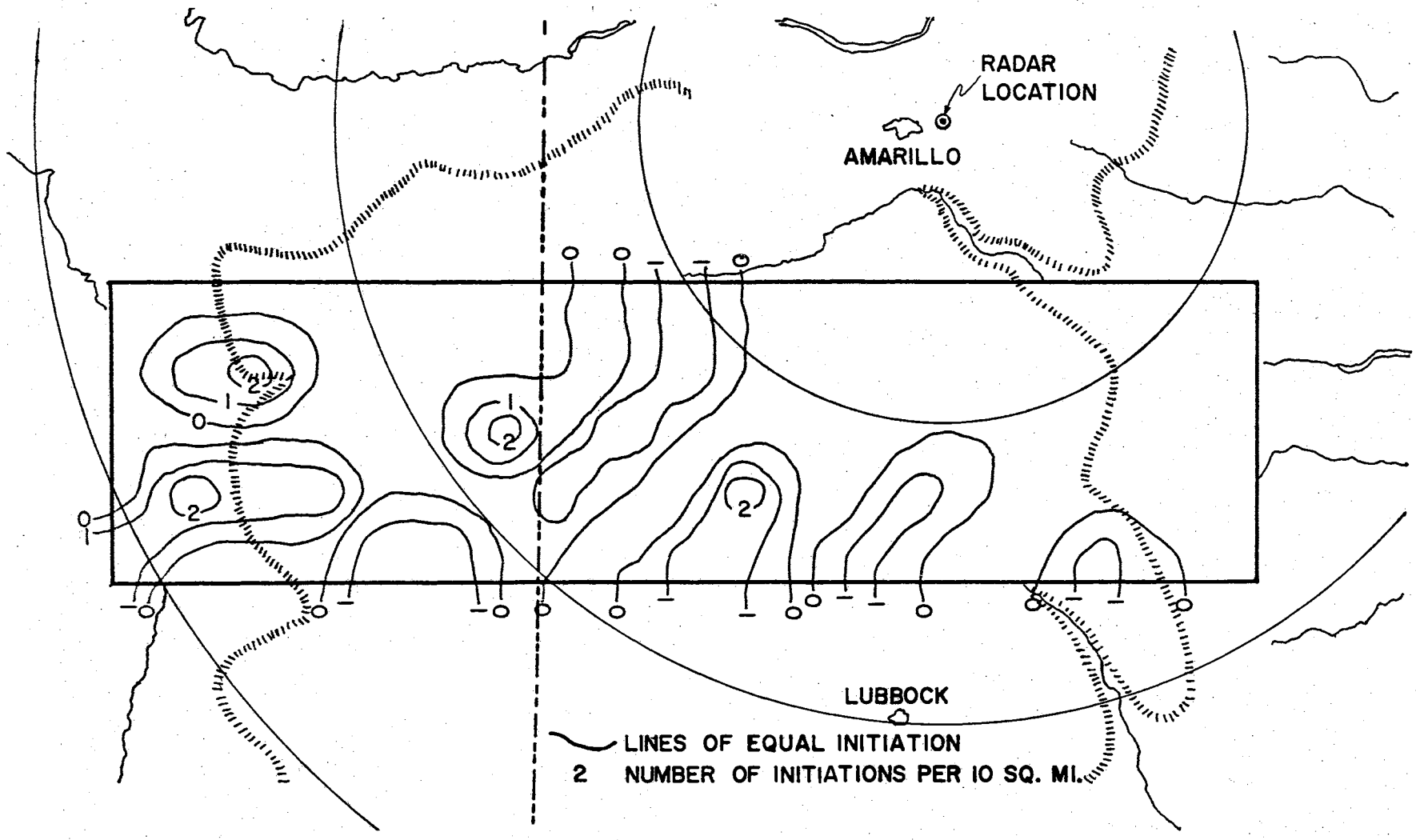

Figure 23. Distribution of locations of initiation for echoes initiating in the study area, June 26-30, 1961.

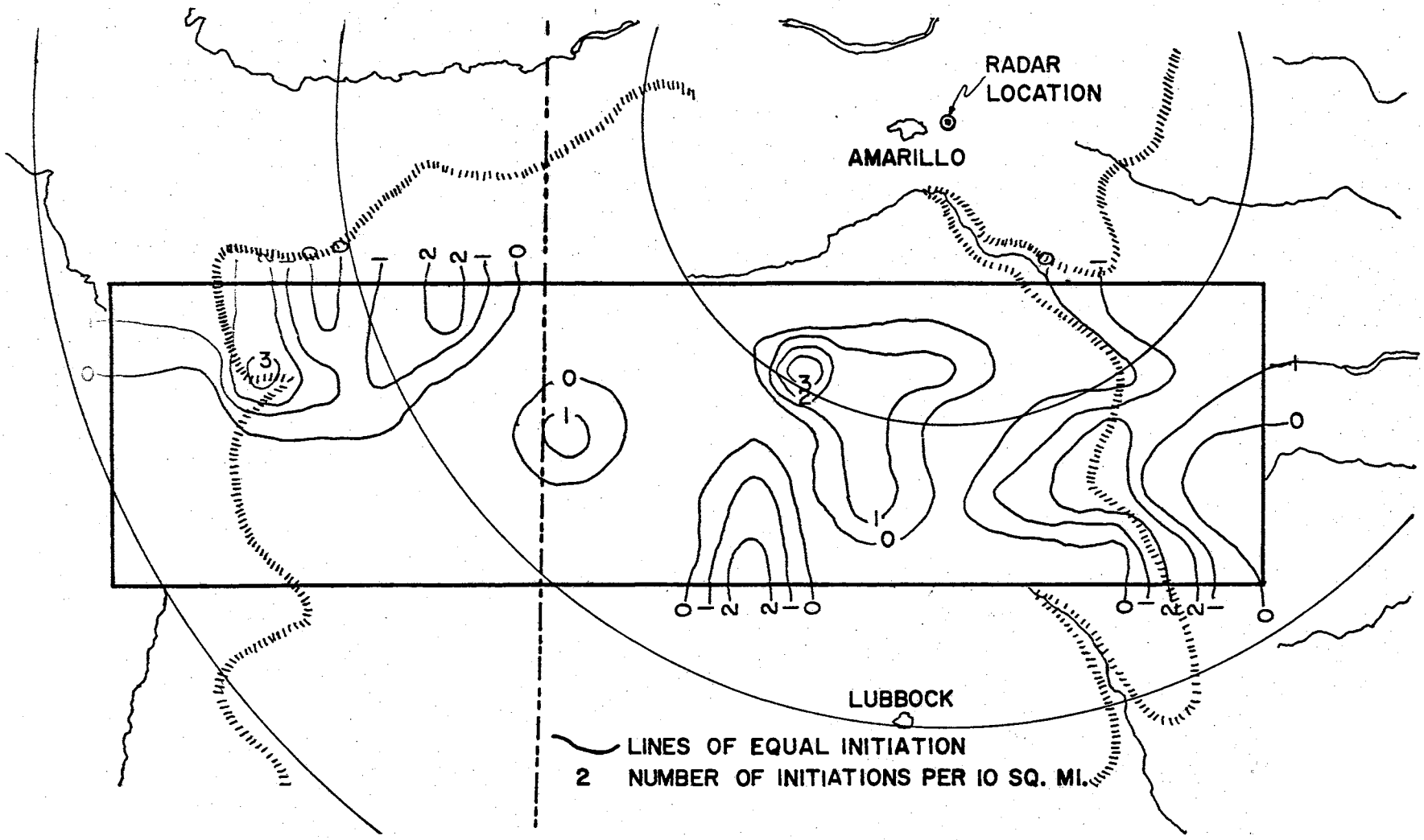

Figure 24. Distribution of locations of initiation for echoes initiating in the study area, July 1-3, 1961.

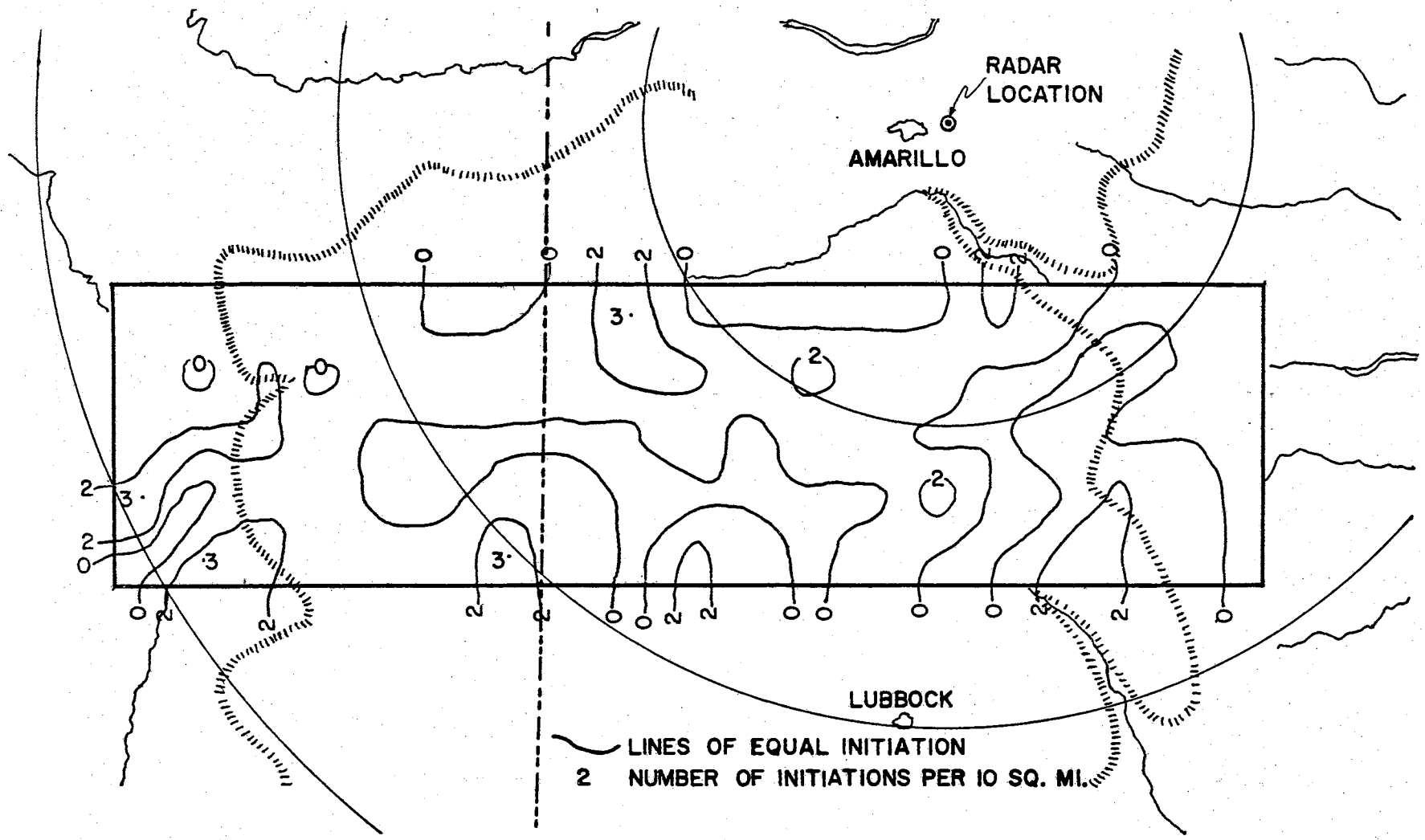

Figure 25. Distribution of locations of initiation for echoes initiating in the study area, July 11-20, 1961.

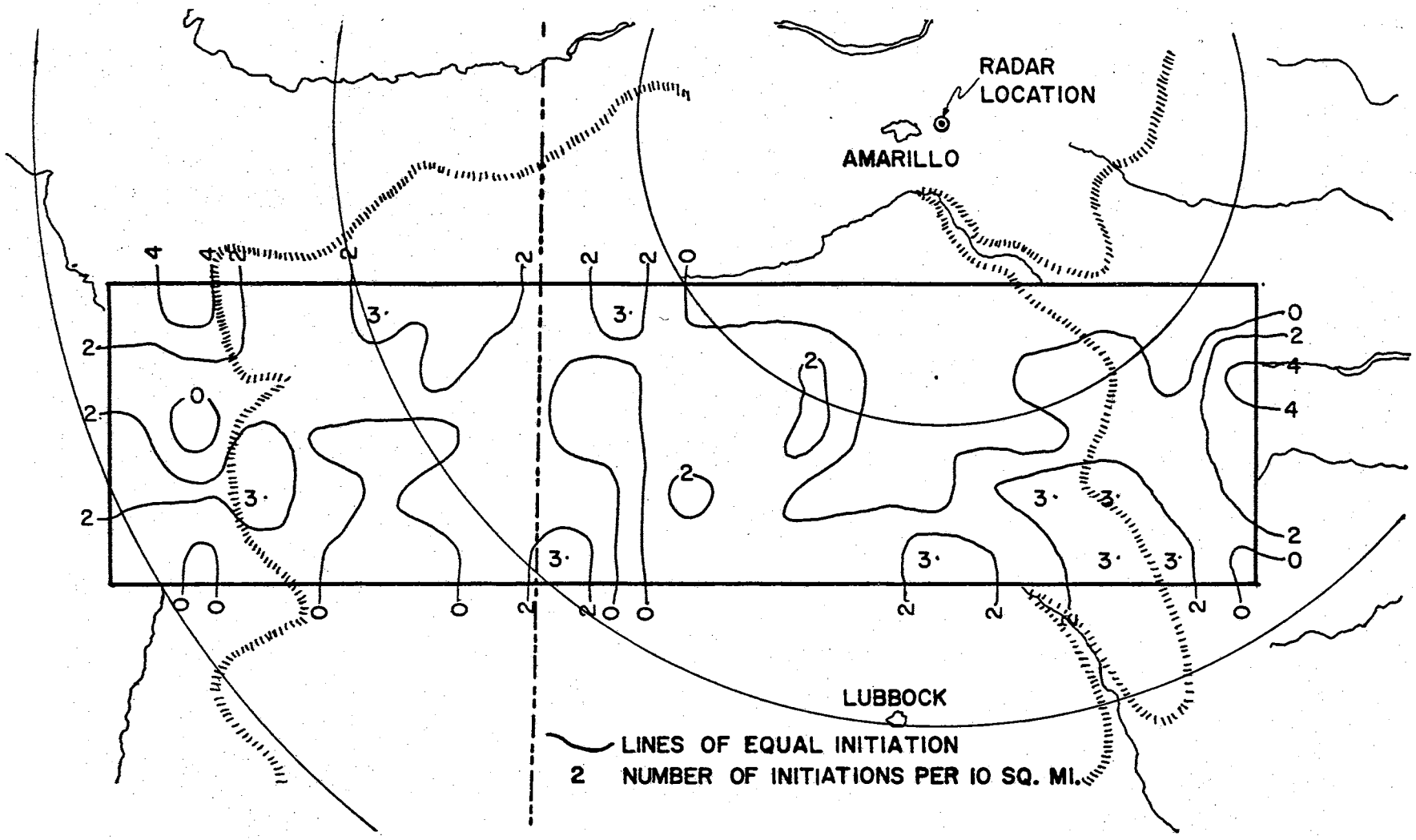

Figure 26. Distribution of locations of initiation for echoes initiating in the study area, August 2-12, 1961.

study were a result of a few echoes consistently initiating there. The prevalent areas for each of the four periods moved during each time interval. They usually did not correspond to the three dominant locations of echo initiation.

The random location of prevalent areas for the four time periods (Figures 23-26) agrees with two well known characteristics of convective thunderstorms.

1. The location of their initiation is random.
2. Once a thunderstorm begins, there is a greater probability of another thunderstorm initiating adjacent to it than at any specified greater distance away. (20).

The second characteristic listed above could result in increased amounts of runoff accumulating in a playa. Since the thunderstorms initiate adjacent to each other, this would increase the possibility that their paths would overlap. Additional amounts of rainfall would then occur on an already saturated soil and runoff would be more likely to occur.

Data such as that presented in Figures 22-26 could assist hydrologists in another manner. The selection of watersheds for studying rainfall-runoff relationships is a complex problem. In addition to considering soil, land use, accessibility, and many other factors, the watershed location must have the same meteorological regime as the area for which data is desired. Radar film for an area under consideration could used to obtain data such as that presented in Figures 22-26 to ascertain the meteorological homogeneity of the area. Then the watershed site would be selected that has the same meteorological regime as the total area for which data is desired.

Echo Area

A frequency distribution of duration weighted, average echo areas is shown in Figure 27. The distribution has unequal area intervals and the discussion concerning the unequal intervals in the duration frequency distribution applies.

The modal average area was 10 to 15 square miles and the median average area was 25 to 30 square miles (Figure 27 and Table X). Ninety percent of the areas were less than or equal to 70 square miles (Figure 28).

Of special interest is the fact that 90 percent of the average areas were equal to or greater than 13 square miles. A thunderstorm can be assumed to be an approximate square according to Byers and Braham. (20). Then, 90 percent of the storms will have an average width equal to or greater than 3.6 miles and 50 percent an average width equal to or greater than 5.4 miles (Figure 28). The watershed of playas were indicated to be normally less than three square miles in area. Therefore, the width of many thunderstorms is greater than the diameter of a playa. Playas centrally located under a thunderstorm will have their watersheds completely covered. The possibility of appreciable amounts of runoff is increased because the playas will have their watershed completely covered by rainfall.

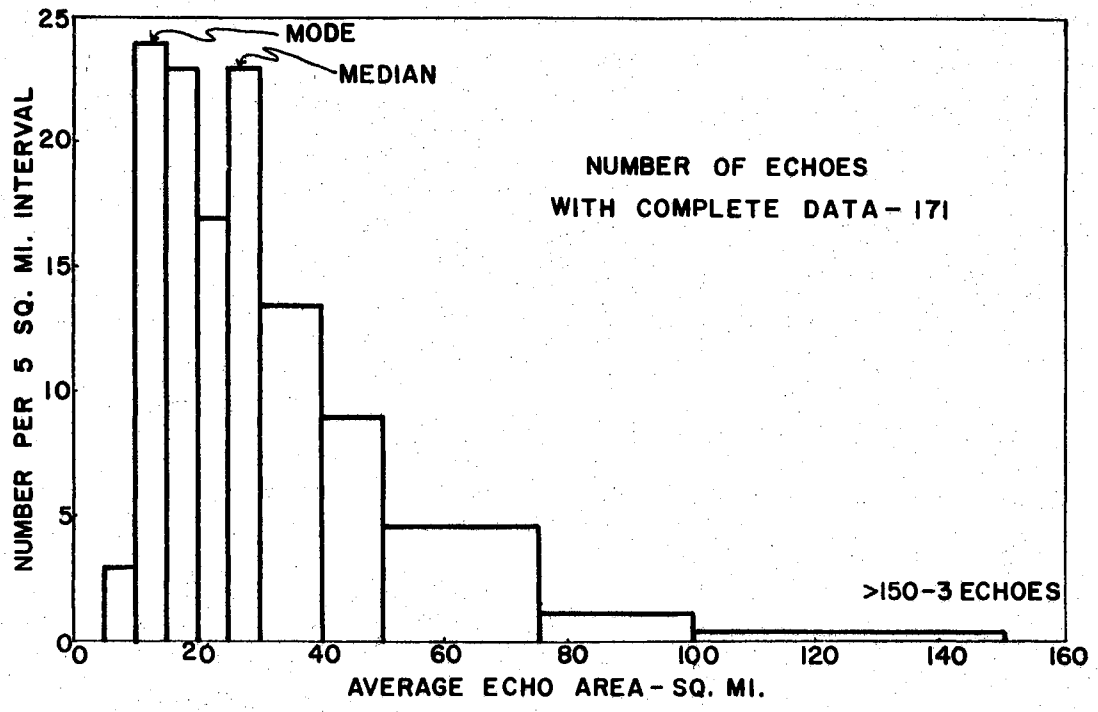

Figure 27. Frequency distribution of average echo areas for indicated intervals of area.

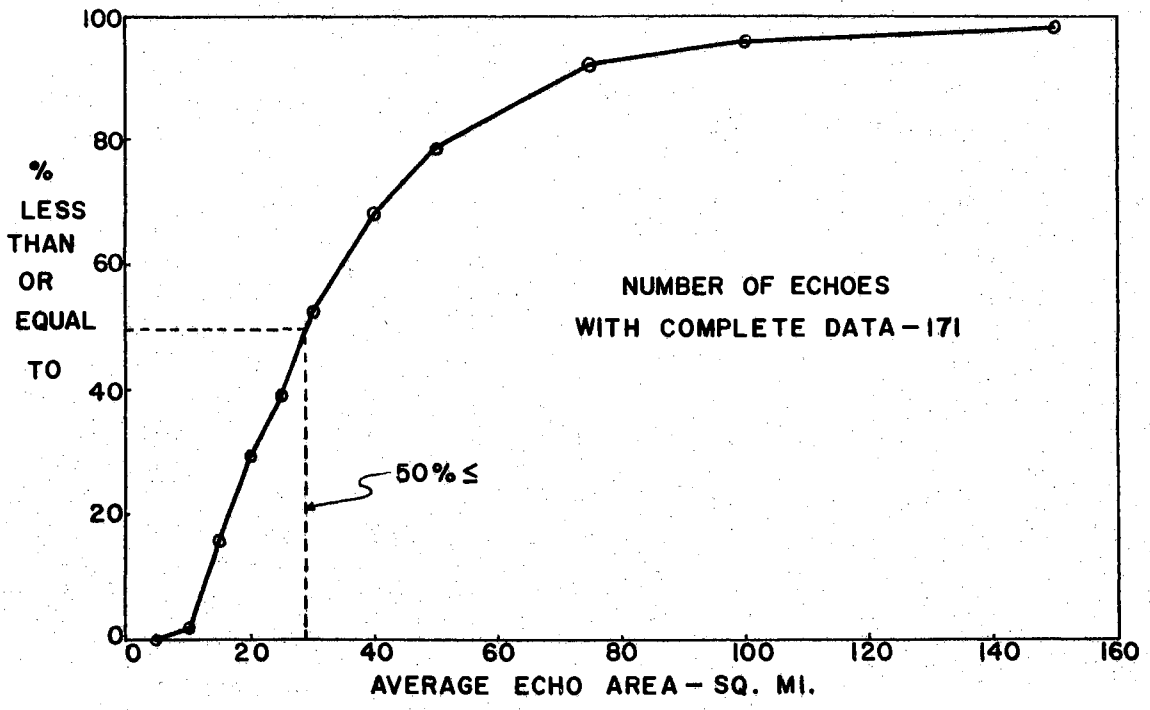

Figure 28. Cumulative percent of total number less than or equal to indicated average area.

TABLE X

DURATION WEIGHTED, AVERAGE AREA OF ECHOES WITH COMPLETE DATA AND FOR INDICATED INTERVALS

Interval (Sq. Mi.)	Number	Accum.	Percent of Total Number Accum.	Number Per 5 Sq. Mi.
$> 0 \leq 5$	0	0	0	0
$> 5 \leq 10$	3	3	1.8	3
$> 10 \leq 15$	24	27	15.8	24
$> 15 \leq 20$	23	50	29.3	23
$> 20 \leq 25$	17	67	38.2	17
$> 25 \leq 30$	23	90	52.7	23
$> 30 \leq 40$	27	117	68.5	13.5
$> 40 \leq 50$	18	135	79.0	9
$> 50 \leq 75$	23	158	92.5	4.6
$> 75 \leq 100$	6	164	96.0	1.2
$> 100 \leq 150$	4	168	98.3	0.8
$> 150 \leq 200$	0	168	98.3	0
$> 200 \leq 300$	2	170	99.5	0.4
> 300	1	171	100.1	0.2

CHAPTER VI

SUMMARY AND CONCLUSIONS

Summary

Patterns of radar echoes of convective precipitation for the High Plains of Texas were studied for 1961. Radar echoes were represented in digital form by a sequence of x,y coordinate readings around the periphery of the echo. The area and centroid of the echo were then computed by a high speed computer utilizing formulas revised or developed by the writer. Duration, distance traveled, speed, direction of movement and other characteristics of the radar echo were then computed and summarized.

Distribution of echo durations revealed the most frequent duration to be from 0.2 to 0.3 hour and the median duration to be 0.6 to 0.8 hour. The median distance traveled was between 0 and 5 miles, but most frequently the echo was stationary. Most prevalent average speeds of echoes was no movement, and the median speed was between 0 and 5 mph.

North and south were the most frequently traveled directions by the echoes, but the two directions were not dominant. Thirty-seven percent of the echoes had no movement. The two peaks of echo initiation during the diurnal cycle occurred during the middle of the afternoon and at midnight. The two peaks correspond to two types of thunderstorms--

daytime thunderstorms that occur during the afternoon due to localized heating, and nighttime thunderstorms that occur due to convergence in the lower levels.

Dominant areas of echo initiation occurred but appeared to vary randomly from one time interval to another. Two of three areas of initiation that were dominant corresponded to the southeastern and northwestern edges of the study area along the escarpment.

A frequency distribution of duration weighted, average echo areas indicated the most frequent area was 10 to 15 square miles and the median area was 25 to 30 square miles.

Conclusions

Conclusions drawn from this study were:

1. Radar echoes of convective precipitation can be converted to digital form and their characteristics computed and summarized by a high speed computer.
2. Most frequent and median characteristics of radar echoes of convective precipitation in the High Plains of Texas were:

Characteristic	Modal	Median	
Duration	0.2-0.3	0.6-0.8	hour
Distance traveled	0	0-5	miles
Average speed	0	0-5	mph
Resultant direction	No movement	-	-
Average area	10-15	25-30	square miles

3. Dominant areas of initiation occur but vary from one time interval to another. Considering all echoes included in the study, two of the three dominant areas of initiation correspond

to the southeastern and northwestern edges of the escarpment in the sample area. Thus, the escarpment appears to furnish enough orographic effect to cause echoes to consistently initiate adjacent to it.

Suggestions for Future Study

Future investigations should determine the year to year variations in precipitation patterns. Relating of echo characteristics to synoptic data should be attempted. Installation of a dense raingage network for a portion of the study area would assist in determining rainfall characteristics of convective precipitation. Future studies of precipitation patterns for the High Plains should include a study of the characteristics of precipitation lines. The proportion of precipitation contributed to the area from convective activity and from precipitation lines needs investigation.

BIBLIOGRAPHY

1. Marshall, J. S., Walter Hitschfeld, and K. L. S. Gunn. "Advances in Radar Weather," Advances in Geophysics. New York: Academic Press, Inc. (1955), pp. 1-56.

2. Battan, Louis J. Radar Meteorology. Chicago: University of Chicago Press, 1949.

3. Marshall, J. S., and W. E. Gordon. "Radiometeorology." Meteorological Monographs, 3(14) (July 1957), pp. 73-113.

4. Austin, Pauline M. "Information Obtainable from Quantitative Observation of Radar Echoes from Precipitation." Proceedings of the Conference on Radio Meteorology. Austin: University of Texas (November 9-12, 1953).

5. Hitschfeld, Walter. "Measurement and Detection of Rainfall by Radar at Attenuating Wavelengths." Proceedings of the Conference on Radio Meteorology. Austin: University of Texas (November 9-12, 1953).

6. Ryde, J. W. "The Attenuation and Radar Echoes Produced at Centimeter Wavelengths by Various Meteorological Phenomena." Meteorological Factors in Radio Wave Propagation. London: The Physical Society, (1946) 169-188.

7. Lord Rayleigh. "On the Scattering of Light by Small Particles." Phil. Mag., 41, (1871) p. 447.

8. Mie, G. "Beitrage Zur Optik Truber Medien, Speziell Kolloider Metallosungen." Ann. Phys., 25(4), (1908) p. 377.

9. Kerr, D. E., Ed. Propagation of Short Radio Waves. New York: McGraw-Hill, 1951.

10. Nupen, W. "Anotated Bibliography of Radar as Applied to Cloud and Precipitation Physics." Meteor. Abstr. Bibliog., 6, (1955) pp. 497-1050.

11. Truppi, Lawrence E. "The Use of Radar Data in the Investigation of Precipitation Distributions and Anomalous Propagation." Unpublished Masters Thesis. College Station, Texas: Texas A & M College, January, 1957.

12. Tarble, Richard D. "The Use of Radar in Detecting Flood Potential Precipitation and Its Application to the Field of Hydrology." Unpublished Masters Thesis. College Station, Texas: Texas A & M College, May, 1957.

13. Clark, Robert A. "A Study of Convective Precipitation as Revealed by Radar Observations, Texas, 1958-59." Journal of Meteorology, 17(4): (August, 1960) pp. 415-425.

14. Changnon, Stanley A., Jr. "Climatological Study of Radar Depicted Lines in the Middle West." Proceedings of the Eighth Weather Radar Conference. San Francisco, California (April 11-14, 1960), pp. 73-80.

15. Truppi, Lawrence E. "Reduction of Radarscope Data to Digital Form." Proceedings of the Eighth Weather Radar Conference. San Francisco, California, (April 11-14, 1960) pp. 459-465.

16. Hildreth, R. J., and G. W. Thomas. "Farming and Ranching Risk as Influenced by Rainfall." Texas Agricultural Experiment Station Miscellaneous Publication 154, January, 1956.

17. Weather Bureau, U. S. Department of Commerce. "Climatological Data New Mexico Annual Summary 1961." 65(13), Asheville: 1962.

18. Jensen, Marvin E., and R. J. Hildreth. "Rainfall at Amarillo, Texas." Texas Agricultural Experiment Station Miscellaneous Publication 583, May, 1962.

19. Ackerman, Bernice. "Characteristics of Summer Radar Echoes in Arizona, 1956." Scientific Report No. 11. Tucson: The University of Arizona, Institute of Atmospheric Physics (July 8, 1959).

20. Byers, H. R., and R. R. Braham. The Thunderstorm. Washington: U. S. Government Printing Office, 1949.

21. Hiser, Homer W., and William L. Freseman. Radar Meteorology. 2nd Edition (1959) (Copyright applied for) Coral Gables, Florida: University of Miami, The Marine Laboratory.

22. Byers, Horace Robert. General Meteorology. 3rd Edition (1959) McGraw-Hill Book Company, Inc. New York, pp. 468-469.

A P P E N D I C E S

APPENDIX A

SAMPLE INPUT DATA FOR COMPUTER

APPENDIX A

SAMPLE INPUT DATA FOR COMPUTER

Echo No.	N + 1	No. of Obs.	No. of Cards	Card Sequence	Year	Month	Day	Hour	Minute	Coordinate	Card No.	Coordinate Values - Miles									
12	13	4	2	1	61	7	13	11	17	X	654	135.0	136.0	137.0	135.0	133.0	131.0	130.0	129.0	129.0	130.0
12	13	4	2	1	61	7	13	11	17	Y	654	10.0	12.0	15.0	017.0	018.0	017.0	015.0	012.0	009.0	007.0
12	13	4	2	2	61	7	13	11	17	X	655	132.0	134.0	135.0	000.0	000.0	000.0	000.0	000.0	000.0	000.0
12	13	4	2	2	61	7	13	11	17	Y	655	6.0	8.0	10.0	000.0	000.0	000.0	000.0	000.0	000.0	000.0
12	17	4	2	1	61	7	13	11	43	X	656	142.0	144.0	144.0	142.0	140.0	139.0	137.0	136.0	134.0	132.0
12	17	4	2	1	61	7	13	11	43	Y	656	10.0	13.0	15.0	017.0	018.0	018.0	017.0	014.0	010.0	007.0
12	17	4	2	2	61	7	13	11	43	X	657	132.0	133.0	135.0	138.0	140.0	141.0	142.0	000.0	000.0	000.0
12	17	4	2	2	61	7	13	11	43	Y	657	6.0	4.0	3.0	003.0	006.0	009.0	010.0	000.0	000.0	000.0
12	10	4	1	1	61	7	13	12	1	X	658	145.0	143.0	141.0	139.0	139.0	140.0	142.0	144.0	145.0	145.0
12	10	4	1	1	61	7	13	12	1	Y	658	10.0	12.0	12.0	010.0	008.0	005.0	004.0	006.0	008.0	010.0
12	0	4	1	1	61	7	13	12	21	X	659	0.	0.		.0	000.0	000.0	000.0	000.0	000.0	000.0
12	0	4	1	1	61	7	13	12	21	Y	659	0.	0.		.0	000.0	000.0	000.0	000.0	000.0	000.0
13	19	5	2	1	61	7	13	16	23	X	660	67.0	69.0	70.0	070.0	069.0	068.0	067.0	066.0	062.0	059.0
13	19	5	2	1	61	7	13	16	23	Y	660	11.0	14.0	15.0	017.0	018.0	019.0	020.0	019.0	017.0	014.0
13	19	5	2	2	61	7	13	16	23	X	661	57.0	57.0	58.0	058.0	059.0	061.0	062.0	064.0	067.0	000.0
13	19	5	2	2	61	7	13	16	23	Y	661	11.0	10.0	8.0	007.0	006.0	005.0	006.0	007.0	011.0	000.0
13	11	5	2	1	61	7	13	17	0	X	662	81.0	82.0	83.0	085.0	085.0	082.0	079.0	075.0	073.0	072.0
13	11	5	2	1	61	7	13	17	0	Y	662	0.	1.0	4.0	007.0	011.0	011.0	009.0	006.0	003.0	000.0
13	11	5	2	2	61	7	13	17	0	X	663	81.0	0.		.0	000.0	000.0	000.0	000.0	000.0	000.0
13	11	5	2	2	61	7	13	17	0	Y	663	0.	0.		.0	000.0	000.0	000.0	000.0	000.0	000.0
13	8	5	1	1	61	7	13	17	22	X	664	87.0	86.0	84.0	081.0	079.0	077.0	077.0	087.0	000.0	000.0
13	8	5	1	1	61	7	13	17	22	Y	664	0.	2.0	4.0	004.0	003.0	001.0	000.0	000.0	000.0	000.0
13	12	5	2	1	61	7	13	17	36	X	665	95.0	94.0	93.0	091.0	088.0	087.0	086.0	084.0	082.0	080.0
13	12	5	2	1	61	7	13	17	36	Y	665	0.	1.0	2.0	003.0	004.0	005.0	005.0	004.0	003.0	001.0
13	12	5	2	2	61	7	13	17	36	X	666	80.0	95.0		.0	000.0	000.0	000.0	000.0	000.0	000.0
13	12	5	2	2	61	7	13	17	36	Y	666	0.	0.		.0	000.0	000.0	000.0	000.0	000.0	000.0
13	0	5	1	1	61	7	13	18	11	X	667	0.	0.		.0	000.0	000.0	000.0	000.0	000.0	000.0
13	0	5	1	1	61	7	13	18	11	Y	667	0.	0.		.0	000.0	000.0	000.0	000.0	000.0	000.0
14	8	3	1	1	61	7	13	17	0	X	668	103.0	101.0	100.0	095.0	092.0	091.0	091.0	103.0	000.0	000.0
14	8	3	1	1	61	7	13	17	0	Y	668	0.	2.0	3.0	003.0	002.0	001.0	000.0	000.0	000.0	000.0
14	10	3	1	1	61	7	13	17	36	X	669	104.0	103.0	102.0	101.0	099.0	098.0	097.0	095.0	095.0	104.0
14	10	3	1	1	61	7	13	17	36	Y	669	0.	2.0	4.0	006.0	007.0	007.0	006.0	004.0	000.0	000.0
14	0	3	1	1	61	7	13	17	52	X	670	0.	0.		.0	000.0	000.0	000.0	000.0	000.0	000.0
14	0	3	1	1	61	7	13	17	52	Y	670	0.	0.		.0	000.0	000.0	000.0	000.0	000.0	000.0
15	7	3	1	1	61	7	13	17	22	X	671	14.0	1.0	3.0	005.0	009.0	011.0	014.0	000.0	000.0	000.0
15	7	3	1	1	61	7	13	17	22	Y	671	50.0	50.0	48.0	047.0	047.0	048.0	050.0	000.0	000.0	000.0
15	11	3	2	1	61	7	13	17	36	X	672	20.0	0.		5.0	006.0	007.0	009.0	014.0	017.0	020.0
15	11	3	2	1	61	7	13	17	36	Y	672	50.0	50.0	42.0	037.0	036.0	036.0	038.0	042.0	045.0	049.0
15	11	3	2	2	61	7	13	17	36	X	673	20.0	0.		.0	000.0	000.0	000.0	000.0	000.0	000.0
15	11	3	2	2	61	7	13	17	36	Y	673	50.0	0.		.0	000.0	000.0	000.0	000.0	000.0	000.0
15	0	3	1	1	61	7	13	17	44	X	674	0.	0.		.0	000.0	000.0	000.0	000.0	000.0	000.0
15	0	3	1	1	61	7	13	17	44	Y	674	0.	0.		.0	000.0	000.0	000.0	000.0	000.0	000.0

APPENDIX B

SAMPLE OUTPUT DATA OF COMPUTER

APPENDIX B

SAMPLE OUTPUT DATA OF COMPUTER

--- PRECIPITATION PATTERNS BY RADAR ECHOES ---

ECHO	N+1	OBS.	YEAR	MONTH	DAY	HOUR	MIN	DELTA TIME	AREA	DISTANCE	X-BAR	SLOPE	Y-BAR	VELOCITY
12	13	4	1961	7	13	11	17		63.0000		132.5793		12.2540	
								0.433		5.78387		250.918		13.349
12	17	4	1961	7	13	11	43		106.5000		138.0454		10.3631	
								0.300		4.39571		242.085		14.650
12	10	4	1961	7	13	12	1		35.5000		141.9296		8.3052	
								0.333		0.		0.		0.
12	0	4	1961	7	13	12	21		0.		0.		0.	
SUMS AND AVERAGES -								0.10666504E 01		0.10179576E 02		0.24710473E 03		0.95434988E 01
13	19	5	1961	7	13	16	23		107.0000		63.3489		12.4907	
								0.617		17.61041		244.277		28.556
13	11	5	1961	7	13	17	0		89.5000		79.2141		4.8473	
								0.367		4.18221		220.957		11.407
13	8	5	1961	7	13	17	22		30.0000		81.9555		1.6889	
								0.233		4.92933		271.597		21.125
13	12	5	1961	7	13	17	36		47.0000		86.8830		1.8262	
								0.583		0.		0.		0.
13	0	5	1961	7	13	18	11		0.		0.		0.	
SUMS AND AVERAGES -								0.17999878E 01		0.26721953E 02		0.24562244E 03		0.14845630E 02
14	8	3	1961	7	13	17	0		28.5000		96.7134		1.3216	
								0.600		2.71955		305.127		4.533
14	10	3	1961	7	13	17	36		45.5000		98.9377		2.8864	
								0.267		0.		0.		0.
14	0	3	1961	7	13	17	52		0.		0.		0.	
SUMS AND AVERAGES -								0.86663818E 00		0.27195549E 01		0.30512706E 03		0.31380510E 01
15	7	3	1961	7	13	17	22		27.0000		7.2099		48.7407	
								0.233		4.17734		196.142		17.903
15	11	3	1961	7	13	17	36		184.5000		8.3713		44.7281	
								0.133		0.		0.		0.
15	0	3	1961	7	13	17	44		0.		0.		0.	
SUMS AND AVERAGES -								0.36663818E-00		0.41773386E 01		0.19614226E 03		0.11393626E 02

VITA

Wayne Clyma

Candidate for the Degree of

Master of Science

Thesis: PATTERNS OF RADAR ECHOES OF CONVECTIVE PRECIPITATION, HIGH PLAINS OF TEXAS, 1961

Major Field: Agricultural Engineering

Biographical:

Personal Data: Born at Keota, Oklahoma, August 1, 1935, the son of Joe, Sr. and Rose Clyma.

Education: Attended grade school and high school at Star and Keota, Oklahoma, respectively. Received the Bachelor of Science degree in Agricultural Engineering in May, 1958, from Oklahoma State University. Completed the requirements for the Master of Science degree in August, 1963.

Professional Experience: Worked the summer of 1955 as student assistant, Agricultural Engineering Department, Oklahoma State University, primarily on small watershed research; summer of 1956 as an engineering aid (student trainee) surveying reservoir sites for the Bureau of Land Management, Farmington, New Mexico; summer of 1957 as an engineering aid (student trainee) in irrigation research, USDA Southwestern Great Plains Field Station, Bushland, Texas; and part time as student assistant Agricultural Engineering Department, Oklahoma State University, in small watershed and evaporation suppression research during the academic year from 1956-1958. Employed since 1958 by USDA, ARS, SWC, Southwestern Great Plains Field Station, Bushland, Texas, as an agricultural engineer in artificial groundwater recharge, irrigation, and surface hydrology research.

Organizations: Member of the American Society of Agricultural Engineers; member of Alpha Zeta, honorary agricultural fraternity; member of Sigma Tau, honorary engineering fraternity.